INVESTIGATION OF HEART RATE VARIABILITY AND BARORECEPTOR SENSITIVITY IN RATS.

by

Harish Ramachandran

for the degree of Master of Research

Department of Engineering
Macquarie University

November 4, 2015

Supervisor: Dr Graham Town

ACKNOWLEDGMENTS

I would like to acknowledge **Professor Graham Town** for sharing his immense knowledge and giving me excellent feedback on my research work as my supervisor and mentor. He provided motivation and guidance during my time spent researching and writing this thesis, especially in signal processing techniques. I would also like to acknowledge **Dr.Mark Butlin** for providing assistance on data manipulation and statistical analysis. I would like to acknowledge **Parissa Kouchaki** for providing me with her experimental results for analysis. Lastly, I would like to acknowledge **Professor Alberto Avolio** for providing me with direction in this thesis.

STATEMENT OF CANDIDATE

I, Harish Ramachandran, declare that this report, submitted as part of the requirement for the award of Master of Research in the Department of Engineering, Macquarie University, is entirely my own work unless otherwise referenced or acknowledged. This document has not been submitted for qualification or assessment at any academic institution.

This thesis aims to critically analyse the results of previously completed rat experiments at the Faculty of Medicine and Health Sciences at Macquarie University. These rat experiments were not undertaken by the author, and the details of any animal experiments are included here only for completeness. Only the results of the experiments were made available for analysis, and is the sole purpose of this thesis.

Student's Name: Harish Ramachandran

Student's Signature:

Date: November 4, 2015

ABSTRACT

Scientific studies have traditionally incorporated pharmacological methods to quantify baroreceptor sensitivity (BRS) in both rats and humans. Baroreceptor stimulation has been shown to be efficacious in lowering blood pressure in clinical trials of patients with drug resistant hypertension. Kouchaki et al [1] showed that carotid field stimulation did not alter acute baroreceptor function gain when vasoactive substances were used to induce changes in blood pressure. This thesis aims to compare the spontaneous BRS and heart rate variability (HRV) in carotid stimulated normotensive and hypertensive rats using time and frequency domain methods without the use of pharmacological agents. BRS and HRV were also investigated in normotensive and diabetic induced rats using time and frequency domain methods. The time domain sequence technique for quantifying BRS was used and it was found in all rats that spontaneous baroreceptor function still persisted. There was a significant difference between the BRS in normotensive and diabetic rats (P<0.05). BRS and HRV were quantified using the Welch periodogram (windowed Fast Fourier Transform (FFT)), Non-Uniform Discrete Fourier Transform (NDFT) and the Lomb-Scargle Periodogram (LSP). It was found that the NDFT, Welch periodogram and the Lomb-Scargle periodogram gave similar results. The respiratory, sympathetic & parasympathetic frequencies influence the low frequency peak of the HRV spectrum in rats. The maximum value of frequency was tracked and is most likely due to the oscillating respiratory component in the rat.

Contents

List of Figures

List of Tables

Glossary

ANS	Autonomic Nervous System
BAT	Baroreceptor Activation Therapy
BP	Blood Pressure
BRS	Baroreceptor Sensitivity
CAN	Cardiovascular Autonomic Neuropathy
CO	Cardiac Output
CNS	Central Nervous System
DAN	Diabetic Autonomic Neuropathy
DBP	Diastolic Blood Pressure
ECG	Electrocardiogram
FFT	Fast Fourier Transform
HF	High Frequency
HR	Heart Rate
HRV	Heart Rate Variability
LF	Low Frequency
LSP	Lomb-Scargle Periodogram
MAP	Mean Arterial Pressure
NDFT	Non-Uniform Discrete Fourier Transform
NO	Nitric Oxide
PI	Pulse Interval
RRI	R to R Interval
RSA	Respiratory Sinus Arrhythmia
SAN	Sino-Atrial Node
SBP	Systolic Blood Pressure

SHR   Spontaneously Hypertensive Rat

STFT   Short Time Fourier Transform

STZ   Streptozocin

SV   Stroke Volume

SVR   System Vascular Resistance

WHO   World Health Organisation

WKY   Wistar-Kyoto Rat

Publications

Ramachandran H, Salum E, Kampus P, Kals J, Town G, Avolio AP, Butlin M. *Barore-ceptor Sensitivity in Diabetic Rats with Treated and Untreated Hypertension.* 38th Annual Scientific Meeting of the High Blood Pressure Council of Australia. Melbourne, Australia. Dec 2-4 2015. (Accepted abstract)

Chapter 1

Introduction

1.1 Blood Pressure

Blood pressure is defined as the force of blood pushing against the walls of the arteries due to the pumping action of the heart (illustrated in Figure 1.1). Hypertension or high blood pressure is a chronic condition where the mean arterial pressure in the arteries are elevated beyond the upper range of the accepted normal range of pressure [2]. The current BP classification is shown in figure 1.2.
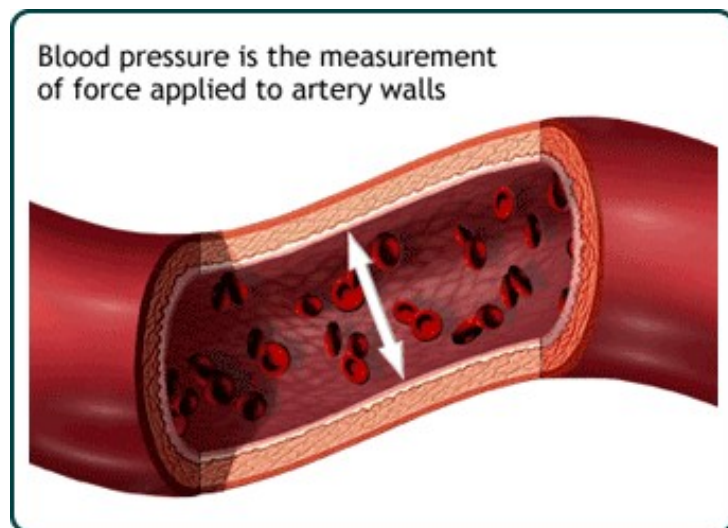
Figure 1.1: Definition of blood pressure. [3]

BP Classification	Systolic BP, mm Hg*		Diastolic BP, mm Hg*	Lifestyle Modification
Normal	<120	and	<80	Encourage
Prehypertension	120-139	or	80-89	Yes
Stage 1 hypertension	140-159	or	90-99	Yes
Stage 2 hypertension	≥160	or	≥100	Yes

Figure 1.2: Classification of blood pressure. [4]

1.1.1 Epidemiology

Hypertension has been identified as one of the most common modifiable risk factors for cardiovascular disease, and lowering blood pressure has been shown to reduce cardiovascular morbidity and mortality [5]. The World Health Organisation (WHO) states hypertension is a major risk factor for ischaemic heart disease and stroke, the two leading causes of death in the world (shown in figure 1.3).

Globally cardiovascular disease accounts for approximately 17 million deaths a year, nearly one third of the total. Of these, complications of hypertension account for 9.4 million deaths worldwide every year. Hypertension is responsible for at least 45% of deaths due to total ischaemic heart disease and 51% of deaths due to stroke [3].
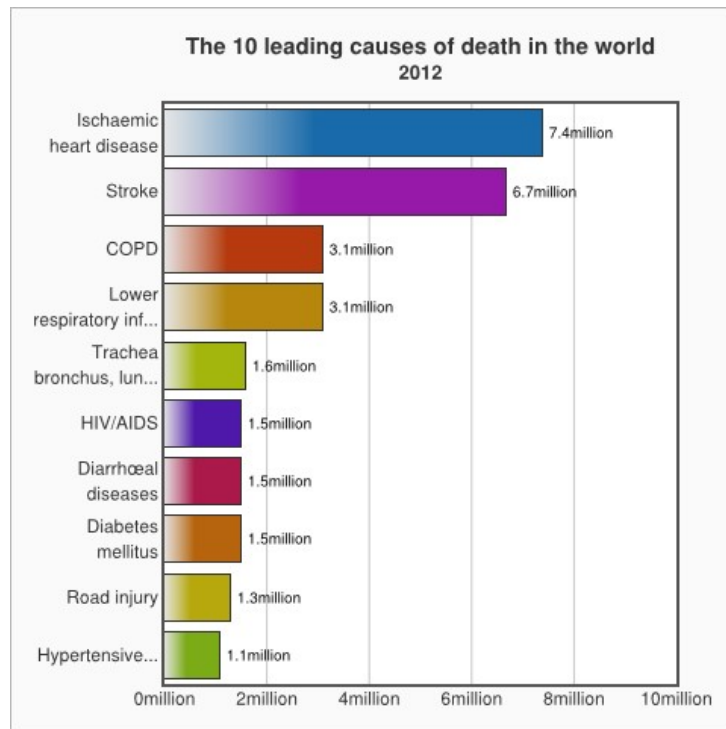
Figure 1.3: Leading causes of death worldwide (2012). [3]

1.1.2 Consequences of Hypertension

Uncontrolled hypertension can cause a number of physiological problems, including:

- Increased workload on the heart: this leads to a plethora of problems including heart failure, coronary heart disease, and an enlarged heart eventually causing heart failure.

- Aneurysms: a bulge in the blood vessels caused by the constant action of high pressure fluid moving through a weakened artery, causing a section to balloon out and possibly rupture causing massive internal bleeding and death

- Strokes: high pressures in blood vessels in the brain can cause damage to the vessel and subsequent death of a major portion of the brain known as a stroke. Strokes can cause paralysis, dementia, blindness or multiple other brain disorders, depending on where in the brain the stroke occurred.

- Kidney damage and failure, uraemia and death [2, 3].

1.1.3 Lowering Blood Pressure

Lowering Blood Pressure can cause significant reductions in risks of strokes and heart attacks regardless of age [6]. The benefits of lowering blood pressure have been shown in clinical trials, where antihypertensive therapy has been associated with 35 % to 40 % mean reductions in stroke incidence; 20 to 25 % in myocardial infarction and more than 50 % in heart failure [7].

1.1.4 Resistant Hypertension

Resistant hypertension is defined as blood pressure that remains high despite treatment with three or more anti-hypertensive treatments of different classes. Ideally, one of the 3 agents should be a diuretic and all agents should be prescribed at optimal dose amounts [8]. A review by Davidson *et al.* (2012) found that carotid baroreceptor stimulation was shown to successfully lower MAP in drug resistant hypertensive patients. The authors concluded that baroreceptor stimulation was an effective adjunct to pharmacological therapies [9].

1.2 Nervous Regulation of Blood Pressure

There are several subconscious nervous control mechanisms that operate all the time to maintain MAP at a normal level. One important mechanism that is responsible for regulating short term arterial pressure is the baroreflex. Simply put, this reflex is initiated by stretch receptors (baroreceptors) located in the wall of several arteries, most importantly the left and right carotid sinus and the aortic arch. A rise in arterial pressure causes the arterial wall to increase in diameter and stretch. This stretch is detected by baroreceptors and as a result, fire action potentials to the cardioregulatory centre in the medulla oblongata. These received signals in the medulla cause an increase in parasympathetic stimulation which cause the inhibition the vasoconstrictor centre and decrease sympathetic stimulation of the heart. This has a two pronged effect: excitation of the baroreceptors causes the arterial pressure to decrease due to a decrease in peripheral resistance(that is, in increase in parasympathetic stimulation) and a decrease in HR (decrease in sympathetic stimulation), which causes a decrease in cardiac output. This lowering of

cardiac output causes a lowering of blood pressure [2].

1.2.1 Baroreceptors and the Baroreflex

The baroreflex is an example of a negative feedback control loop in the human body. This loop consists of the following elements [10]:

1. **Detector**: this is a sensor or receptor which measures the controlled variable and tranduces it into an electrical signal. In the case of the baroreflex, the sensors would be the baroreceptors themselves. It is to be noted here that baroreceptors are stretch sensitive receptors: A increase in transmural pressure due to higher blood volume enlarges the artery and deforms the receptors. Direct stretching of the receptor results in increased firing of the baroreceptors sensory nerve. The baroreceptors encode the mechanical response as a frequency modulated signal.

   Thus, baroreceptors are an example of mechanotransduction, where a cell converts mechanical deformation into electrician impulses.

2. **Afferent neural pathways**: Convey messages from the detector to the central nervous system. The baroreceptors in the carotid sinuses send electrical impulses through the glossopharyngeal nerve (IX cranial nerve), which then relays the signal to the cardioregulatory centre in the medulla oblongata (specifically, the nucleus tractus solitarus).

3. **Coordinating centre**: A control centre in the CNS compares the detected action potentials to a reference signal and generates an error signal. It then sends out action potentials via parasympathetic fibres the appropriate effector organs. In the case of the baroreflex, the cardioregulatory centre is the control centre which compares the incoming action potentials to a reference blood pressure signal and sends out an appropriate set of action potentials if a positive error signal(i.e. high blood pressure) is detected.

   If high blood pressure is detected, the vasoconstrictor centre of the medulla is inhibited.

4. **Efferent neural pathways**: Convey responses from the CNS to the periphery.

In the case of the baroreflex, there is a two pronged effect: efferent signals travel via parasympathetic nerve fibres of the vagus nerve which project onto the heart. This has the effect of decreasing HR.

Sympathetic inhibition occurs to decrease peripheral resistance, that is, vasodilation of arteries/arterioles and veins. This feedback loop is illustrated in figure 1.4:
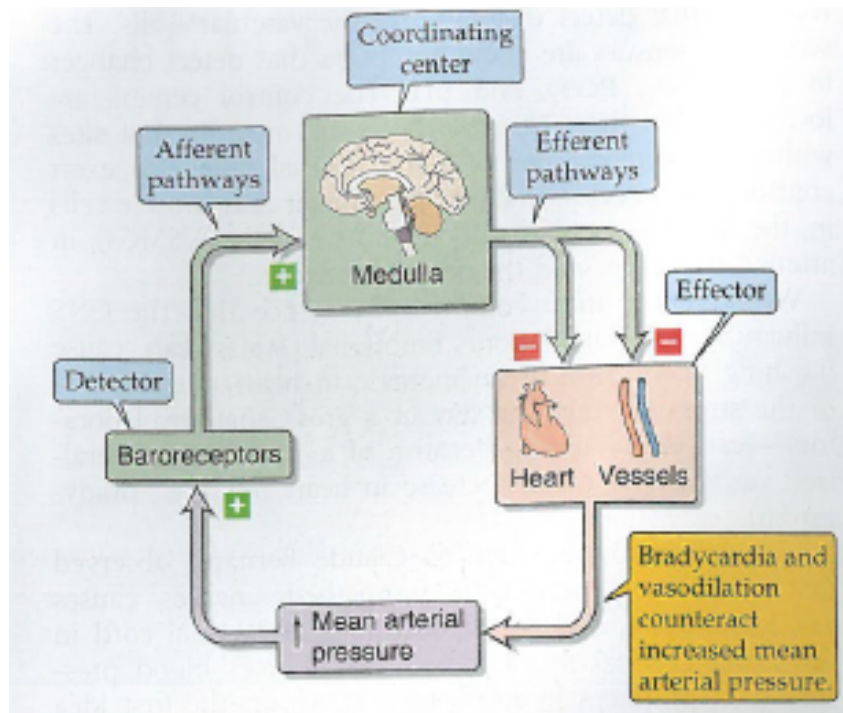
Figure 1.4: Baroreceptor feedback loop. This example looks at an increase in BP.Figure taken from [10]

.

Of course, a lowering of blood pressure has the effect of sympathetic activation and parasympathetic inhibition. This has the effect of increasing HR (sympathetic activation) and thus increasing cardiac output. Decreased vagal tone leads to a higher systemic vascular resistance (SVR). These two factors cause blood pressure to rise. This feedback system is illustrated in figure 1.5 below.

Baroreceptors respond to acute changes in blood pressure. There is some controversy about their importance in regulating long term blood pressure. One reason is that barore-
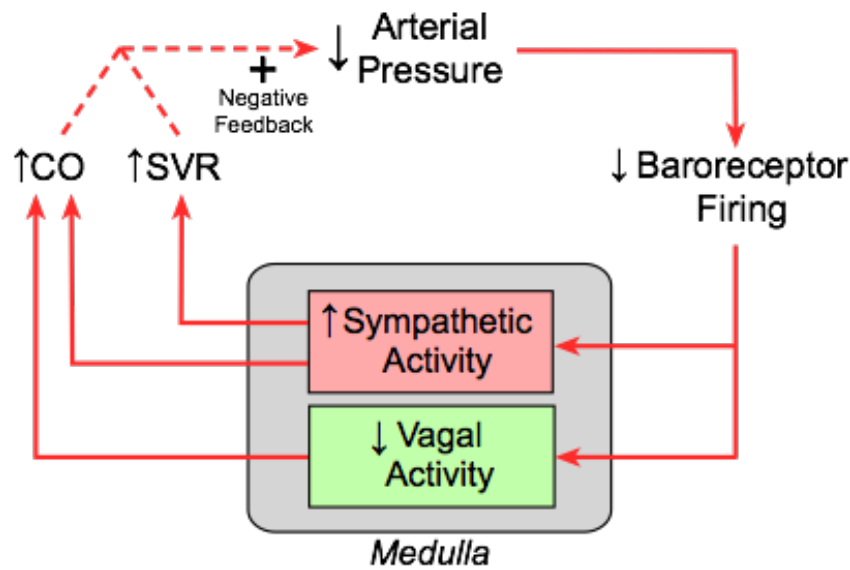
Figure 3. A sudden decrease in arterial pressure decreases baroreceptor firing, which activates sympathetic neurons and inactivates vagal neurons in the medulla. The resulting increases in CO and SVR act as a negative feedback mechanism to attenuate the fall in arterial pressure.

Figure 1.5: Baroreceptor feedback loop. This example looks at a decrease in BP. Figure taken from [11]

.

ceptors are adaptable to new baselines. Baroreceptors tend to reset to a new pressure they are exposed to after 1-2 days [2]. A decrease in baroreceptor sensitivity occurs in hypertension when the carotid sinus becomes stiffer and less deformable due to high intra-arterial pressure. Thus a new baseline is set. The set point of the baroreceptor is raised so that the threshold is increased and the receptors are less sensitive to change in transmural pressure [12].

1.3 Diabetes and Hypertension

There is a significant correlation between diabetes and hypertension, with the two diseases frequently occurring together. Hypertension is a common comorbid condition in patients with type 1 or type II diabetes. Hypertension accelerates the course of complications of diabetes and hypertension most often precedes type II diabetes and vice versa. The diabetes / hypertension disease combination strongly predispose a person to

atherosclerotic cardiovascular disease. The exact pathophysiological link between these two diseases is multifaceted and still under investigation. It is thought that there these two diseases are associated with an impairment of endothelium vasorelaxation. A lack of bioavailability of nitric oxide (NO), a potent vasodilator has been observed in comorbid diseases such as heart failure, diabetes and hypertension [13].

1.3.1   Diabetes and BRS

A reduced BRS has been demonstrated in subjects with diabetes mellitus both in experimental models using streptozotocin (STZ)-induced diabetic rats and in diabetic patients [14]. Diabetic autonomic neuropathy (DAN) is a serious complication of diabetes where organ innervating nerve fibres are damaged. The exact mechanism of neural injury is not clear, but it has been hypothesised that the nerve injuries are due to chronic hyperglycaemia, causing a cascade of events leading to neve injury. Cardiovascular autonomic neuropathy (CAN) is a form of DAN characterised by damage to the autonomic nerve fibres innervating the heart and blood vessels. An impairment in BRS is a consequence of CAN [14].

1.4   Heart Rate Variability: Definition and Origins

Heart rate variability (HRV) is the natural variations in instantaneous HR. The beat-to-beat fluctuations reflect the dynamic response of the CV system to naturally occurring perturbations in the body, such as variations in intrathoracic pressure due to respirations and blood pressure changes that are regulated by the baroreceptors and chemoreceptors. HRV is one the key indicators of autonomic activity in the body, along with BRS. A high HRV is found in hearts with good function, whereas HRV is decreased with severe coronary artery disease, congestive heart failure, aging and diabetic neuropathy. It continues to be a significant predictor of mortality after an acute myocardial infarction [15]. HRV is the variation in length of RR intervals in consecutive heartbeats due to extrinsic regulation of HR. The baroreflex is a negative feedback mechanism which regulates short term blood pressure and is one mechanism which gives rise to HRV. Heart rate variability can be caused by several mechanisms, outlined below.

1.4.1 Autonomic Control of Heart Rate

The normal rhythm of the heart is controlled by the electrical impulses of the sinoatrial node in the right ventricle. The SA node is modulated by innervation from both the sympathetic and parasympathetic divisions of the autonomic nervous system (ANS). The nervous pathway of both branches of the ANS consists of two sets of neurons arranged in series. Their structure consists of preganglionic neurons which originate in the CNS and terminate in the peripheral ganglia, and postganglionic neurons innervating the target organs [16].

The Sympathetic Nervous System

Sympathetic nerve fibres stimulation is an increase in firing of electrical impulses via sympathetic neural pathways. Sympathetic stimulation occurs in response to stress and exercise (the fight or flight response). An increase of firing of sympathetic nerve fibres causes the increase of firing rate of pacemaker cells in the SA node, causing an increase in HR. The exact mechanism is due to the release of catecholamines acting on cardiac beta-1 receptors have positive ionotropic and chronotropic effects [16].

The Parasympathetic Nervous System

Parasympathetic nerve fibre stimulation is an increase in firing of electrical impulses via parasympathetic neural pathways. Parasympathetic stimulation occurs in response to regulate the bodys unconscious activities. These activities are sometimes referred to as rest-and-digest or feed and breed activities, and include activities such as digestion, urination, defecation, salivation, lacrimation, sexual arousal and function of internal organs. An increase of firing of parasympathetic nerve fibres causes a decrease in HR. The exact mechanism is due to the release of the neurotransmitter acetylcholine by parasympathetic nerve terminals. Acetylcholine binds to muscarinic receptors, causing a decrease in cardiac pacemaking [16].
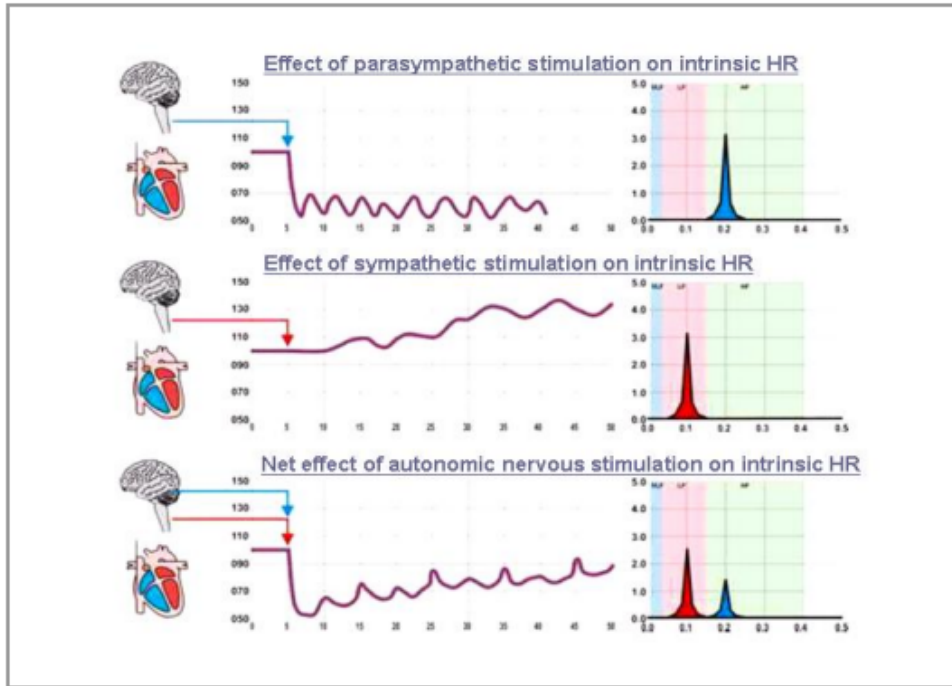
Figure 1.6: Both sympathetic and parasympathetic stimulation affect HR on different time scales. The heart response time to parasympathetic stimulation is almost instantaneous. In contrast, sympathetic effects are quite slow. According to Medicore's 'HRV Analysis System' pamphlet, it takes about 5 seconds to increase HR after onset of sympathetic firing. Figure taken from [17].

1.4.2 Respiratory Sinus Arrythmia

Respiratory sinus arrhythmia (RSA) is the heart rate varying synchronously with respiration, by which the R-R interval on an ECG is shortened during inspiration and lengthened during expiration.

1.4.3 Other Factors Affecting HRV

Humoral mechanisms, such as the renin-angiotensin system, hormonal and reflex control (such as thermoregulation, chemoreflex) are all contributing factors to HRV, albeit these factors affect HRV on a slower time frame. It is to be noted that sympathetic and parasympathetic stimulation are the primary mechanisms which causes rapid changes in HR. This thesis will focus primarily on the nervous control of HRV along with RSA [18].

1.5 Neurostimulation Devices

Neurostimulators are devices which can detect changes in a physiological signal, and respond by delivering an appropriate pulse(s) to the patient in real time. Some examples of neurostimulators include the vagus nerve stimulator from Cyberonics, which stops epileptic seizures from forming [19]. The company's AspireSR neurostimulator looks at the fact that seizures affect the neural circuitry regulating the heartbeat; that is to say, the patient's heartbeat begins to race as a seizure commences. The device measures the heart's electrical activity with an ECG sensor and extracts heartbeat signals. A feedback loop compares the last few seconds of data with the prior few minutes of data to differentiate sudden spikes in ECG from gradual increases. The sudden spikes would be due to the start of a seizure, whereas gradual increases could be due to exercise or excitement. If a seizure is detected, the device delivers a pulse of electricity through electrodes wrapped around the vagus nerve to stop the seizure from happening [19].

1.5.1 Baroreflex Activation Therapy

Baroreflex Activation Therapy (BAT) is the use of electric stimulation of the carotid sinus for the treatment of resistant hypertension. Several clinical trials have been conducted to determine the safety and efficacy of such a neuromodulation device.

The study of Scheffers et al. (2010) [20] looked at the safety and efficacy of a baroreceptor electrical stimulation device, the CVRx Rheos Hypertension Therapy System. This was a first-in human evaluation study which investigated the efficacy of baroreceptor activation therapy in a double-blind, randomised placebo controlled clinical trial. The device was implanted in 265 patients with resistant hypertension. They were subsequently randomized 1 month after implantation. Subjects received either BAT (Group A) for the first 6 months or delayed BAT therapy after 6 months (Group B). The trial showed significant benefit for the endpoints of sustained efficacy of baroreceptor activation therapy in both groups.

Another study into the Rheos Hypertension Therapy System was investigated. Forty-five hypertensive subjects with systolic blood pressure > 160 mmHg or diastolic > 90

mmHg were enrolled in a non-randomized feasibility study to assess the efficacy of the Rheos Hypertension Therapy System by CVRx. Subjects were followed up for as long as 2 years. After 3 months of device therapy, mean arterial pressure was reduced by 21/12 mm Hg. This result was persistent in 17 subjects who completed 2 years of follow-up, with a mean reduction of 33/22 mm Hg [21].

From the various studies completed, one can conclude that there is hope with resistant hypertensive patients in the form of baroreceptor activation therapy.

1.5.2   BAT and Tolerance

Studies have also investigated whether or not patients can build up a tolerance to chronic use of Baroreceptor Activation Therapy (BAT). In an American Heart Association conference presentation in 2013, researchers investigated whether long term chronic baroreceptor stimulation influences the acute responsiveness to stimulation. 12 resistant hypertensive patients were recruited in a study which investigated the on/ off effects of BAT at different time points after implantation. They were implanted with the Barostim Neo device by CVRx Inc. For on/off testing three BP measurements were taken at an average of 13.6 months after implant activation at the following intervals: after 5 minutes of rest with the activated device, 5 minute after deactivation of the device, 5 minute after reactivation of the device.

The investigators found that unilateral baroreceptor activation therapy reduces BP consistently in patients with resistant hypertension. They found that acute on/off response to BAT is the same in patients with long term BAT as it is with those patients with recent device activation. They found no evidence of tolerance over time to chronic BAT [22].

1.5.3   Unilateral vs Bilateral Stimulation

Questions have also been raised over the effectiveness of unilateral stimulation to bilateral stimulation of the carotid baroreceptor, and whether stimulating the right or left baroreflex complex had more potential to reduce blood pressure.

A recent study investigated whether unilateral stimulation would produce comparable results as bilateral stimulation. Unilateral stimulation was applied unless bilateral stimulation resulted in a greater blood pressure reduction.

The trial had 215 patients who received BAT on one side only. 127 patients were stimulated on the left carotid sinus, with 88 being stimulated on their right side. 80 patients had been stimulated bilaterally. After 6 months of stimulation, the researchers found that unilateral and in particular right-sided BAT had a more profound effect in reducing blood pressure than bilateral or left-sided BAT [23].

1.6 Stimulation of Hypertensive Rats

Kouchaki *et al.*(2014) investigated whether persistent electric field stimulation of the baroreceptor complex changes baroreceptor function. Figure 1.7 shows the electric field setup that was used:
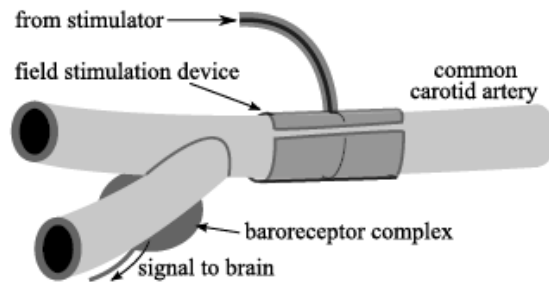
Figure 1.7: A schematic of the baroreceptor field stimulation: The positive electrode of the field was placed around the common carotid artery. There is no direct contact with the baroreceptor complex or nerve, with stimulation being achieved through an electrical field. A negative electrode was placed near by and close to the body surface to complete the electric field. Figure taken from [1].

Unilateral field stimulation was applied to spontaneously hypertensive rats (SHR) for a period of 30 minutes. An example of stimulation is shown in figure 1.8. A vasoconstrictor substance was administered to induce a change in MAP. Baroreceptor function was measured by quantifying HR response to changes to MAP. It was found that field stimulation of the carotid baroreceptor reduced HR and MAP significantly, and stimulation did not affect the acute baroreceptor function peak gain; there was no significant difference

between the peak gains at baseline (no stimulation) and during stimulation. Baroreceptor gain measurements is illustrated in figure 1.10.
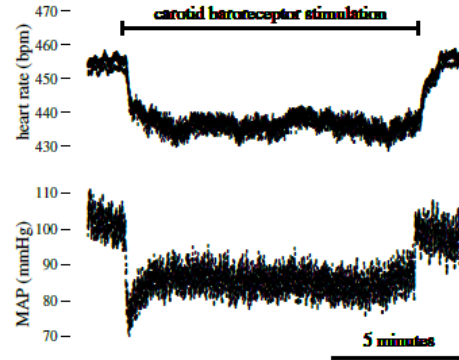
Figure 1.8: An example of field stimulation of the carotid baroreceptors for approximately a 10 minute period. HR and MAP show a rapid change upon activation and de-activation of stimulation with MAP being relatively stable during the stimulation period. Stimulation was at a frequency of 100 Hz, with a 0.53 ms pulse width. Pulse amplitude in this case was 3.2 V. Figure taken from [1].

Unilateral field stimulation of the carotid baroreceptor complex served to reduce the baseline of the MAP and HR. When a vasoconstrictor substance like phenylephrine is administered, it was found that baroreceptor function was preserved, with a reduction of HR and MAP. Figure 1.9 illustrates this.

Because baroreceptors are located in both carotid arteries and in the aortic arch, it may well be that baroreflex function is preserved by signals from the aortic arch and carotid baroreceptors that are not stimulated [1].
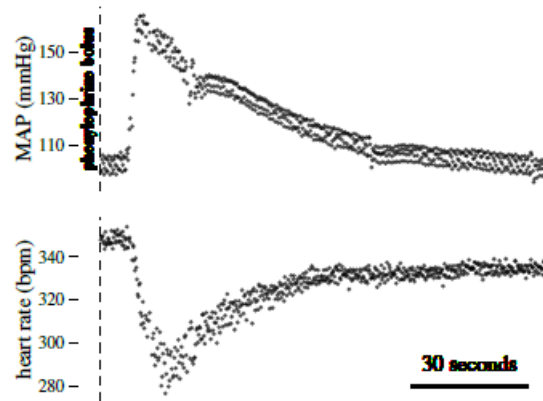
Figure 1.9: Example data showing the effect of an intravenous bolus of phenylephrine (PE) on mean arterial pressure (MAP) and the resulting reduction in HR due to the baroreceptor response. Each point represents a single pulse. Description and figure taken from [1].
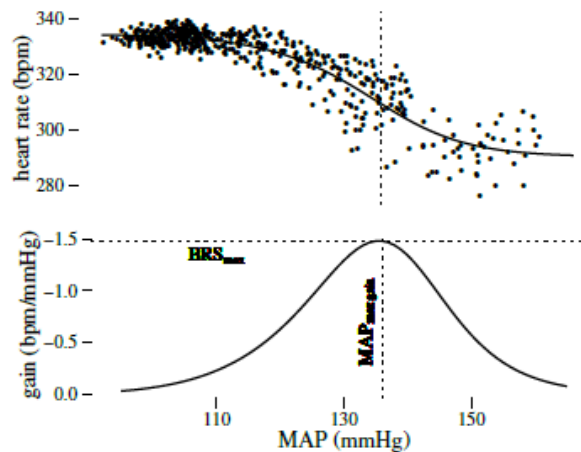
Figure 1.10: A typical baroreceptor response to a blood pressure fall following the pressure rise induced by a bolus injection of phenylephrine. The baroreflex negative feedback loop causes decreasing HR with increasing pressure (or vice-versa). The maximum slope, or gain that occurs at the inflection point is indicated by the dashed line. The MAP and HR at which this occurs is indicated by the dotted lines. Baroreceptor gain (lower panel) is expressed as the absolute change in heart rate relative to change in MAP. Figure taken from [1].

1.7   Novelty of Study and Project

The paper by Kouchaki *et al.* (2014) described is novel in its field because it is the first study to demonstrate preserved baroreceptor function during (unilateral) field stimulation of the carotid baroreceptor complex using vasoactive substances to induce changed in blood pressure.

Baroreceptor function was quantified by the peak gain of the slope of the MAP vs. HR graph, and the peak gain is found at the inflection point. The maximal baroreceptor gain without stimulation was -1.20±0.41 bpm/mmHg and during stimulation -1.41±0.52 bpm/mmHg (p=0.59). Thus it was found that the baroreceptor field stimulation did not alter acute baroreceptor function peak gain.

It is hypothesised that during stimulation, the single baroreceptor complex is electrically saturated, and thus there is a reduction of baseline HR and MAP. When a vasoactive substance is introduced, alternate baroreceptor sites such as the aortic arch and the other unstimulated carotid receptor complex provide the necessary feedback loop to lower blood pressure.

1.8   Justification and Purpose of Research

The purpose of this study is to quantify BRS and HRV in control and diseased rats using time and several frequency domain techniques. This project has several sets of data that are to be analysed differently and for different purposes. The details are outlined as follows:

1. **BRS and HRV Quantification in SHR and WKY Rats**

   The first set of data available is a set of BP and HR measurements for both unilaterally stimulated & non-stimulated SHR rats and WKY rats (control strain). This project aims to quantify the BRS and HRV in both control and hypertensive strains (stimulated and non-stimulated) by using the time domain sequence technique. There is no pharmacological agents administered to elicit a baroreceptor response; the aim of the sequence technique is to investigate the function of barore-

ceptors in both strains. Appendix A lists the Matlab code for both baroreceptor activation (positive sequences) and baroreceptor deactivation (negative sequences) for a set of data. HRV will be calculated in the time domain using the standard deviation of normal-to-normal intervals of the ECG signal (SDNN). BRS and HRV quantification will also be done in the frequency domain, using several frequency techniques to calculate the low frequency and high frequency α-coefficients. These frequency techniques are: (1) the Non-Uniform Discrete Fourier Transform (NDFT), (2) the windowed Fast Fourier Transform (FFT), (3) the Lomb-Scargle Periodogram.

From the previous work of Kouchaki et al, it is hypothesised that spontaneous sequences will be detected in WKY and SHR rats with and without stimulation. It is hypothesised that the BRS will be the same within strains before and after stimulation. It is also hypothesised that calculation of BRS in the time and frequency domains will be similar, since they have the same units of ms/mmHg.

The HRV measurement will be investigated between stimulated and non-stimulated strains.

2. **BRS and HRV Quantification in Wistar and Diabetic Rats**

This project aims to quantify the BRS and HRV in both control(wistar) and diabetic strains by using time and frequency domain techniques.HRV and BRS will be calculated in the time and frequency domain using the measurement techniques mentioned in aim 1.

It is hypothesised that there will be a decrease in HRV and BRS in diabetic rats.

Chapter 2

Measures of HRV and BRS

A combined task force consisting of the European Society of Cardiology and the North American Society of Pacing and Electrophysiology set out to create standards to measure HRV using various techniques. These techniques are used as the gold standard today, and include both time, frequency and geometric methods of calculating HRV. The complete list of techniques can be found within reference [24]. Table 2.1 and table 2.2 shows the gold standard time and frequency domain methods used to quantify HRV:

Table 2.1: Table showing various time domain methods of quantifying HRV. Table taken from [24].

Variable	Units	Description
Statistical Measures		
SDNN	ms	Standard deviation of all NN intervals
SDANN	ms	Standard deviation of the averages of NN intervals in all 5 - minute segments of the entire recording
RMSSD	ms	The square root of the mean of the sum of the squares of differences between adjacent NN intervals
SDNN index	ms	Mean of the standard deviations of all NN intervals for all 5-minute segments of the entire recording
SDSD	ms	Standard deviation of difference
NN50 count		Number of pairs of adjacent NN intervals differing by more than 50 ms in the entire recording; three variants are possible counting all such NN intervals pairs or only pairs in which the first of the second interval is longer
pNN50	%	NN50 count divided by the total number of all NN intervals

2.1 Measuring HRV in the Time Domain

Table 2.1 outlines the methods that are used to calculate the HRV in the time domain. The simplest one is taking the SDNN, the standard deviation of normal-to-normal intervals. The reliability of SDNN depends on the length of the recording period. Typically, the SDNN is calculated over a 24-h period and encompasses both short and long term variations in HRV. It is innapropriate to compare SDNN measures obtained from recordings of different durations. This thesis deals with recording that are on the order of magnitude of a couple of minutes, and thus, the SDNN measures short term variability of heart rate. In is therefore an acceptable standard of measure in this study.

Table 2.2: Table showing various frequency domain methods of quantifying HRV, with typical frequency ranges for humans. Table taken from [24].

Variable	Units	Description	Frequency Range
Analysis of Short-term Recordings (5 mins)			
5- min total power	ms^2	The variance of NN intervals over the temporal segment	$\approx \leq 0.4$ Hz
VLF	ms^2	Power in VLF range	≤ 0.4 Hz
LF	ms^2	Power in LF range	0.04 -0.15 Hz
LF norm	nu	LF power in normalized units LF/(total power-VLF) $\times$ 100	
HF	ms^2	Power in HF range	0.15 -0.4 Hz
HF norm	nu	HF power in normalized units HF/(total power -VLF) $\times$ 100	
LF/HF		Ratio LF[ms^2]/HF[ms^2]	

2.2 Measuring BRS in the Time Domain: The Sequence Technique

The sequence technique was first introduced by Bertieneri *et al.*(1988) [26] as a new approach to quantify baroreceptor function. They stated that the widely employed method for studying the baroreflex by injecting a vasoactive substance has its limitations, namely:

- The reproducibility of the reflex response is far from optimal.

- changes in the reflex response by direct action of the vasoactive drugs on different components of the reflex arch (baroreceptors, integrating centres and sino-atrial node) cannot be ignored.

- the artificially induced stimuli only poorly mimic the naturally occurring pressor and depressor responses.

The sequence technique is a time domain method based on the computational identification of spontaneously occurring sequences of 3 or more consecutive beats characterised by either a progressive rise in systolic blood pressure (SBP) and concomitant increase

in R-R interval time (+RR/+SBP sequence) or by a progressive decrease in SBP and concomitant shortening in R-R interval (-RR/-SBP sequences). In this way, the sequence technique aims to quantify the body's natural baroreflex response without the use of external pharmacological agents.
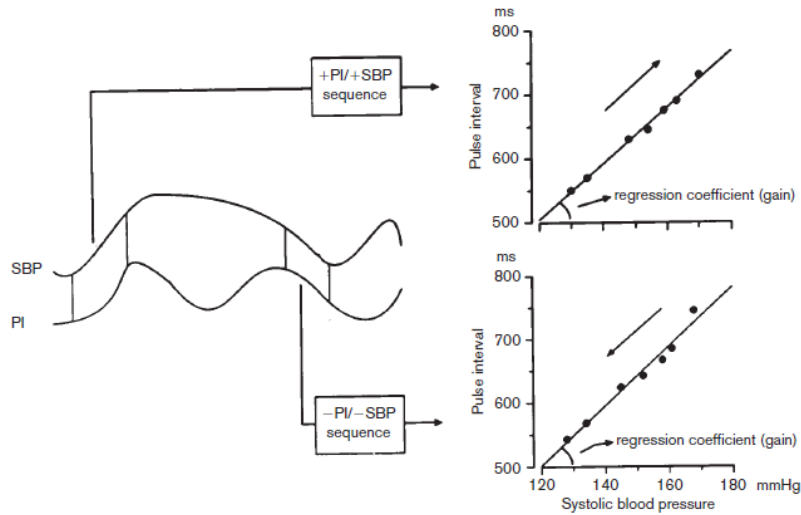
Figure 2.1: A conceptual illustration of how the sequence technique is calculated. Positive sequences (tachycardia) involves the identification of 3 or more consecutive increasing SBP pulses, with a concomitant increase in R-R interval. Negative sequences(bradycardia) involves 3 or more consecutive decreasing SBP pulses, with a concomitant decrease in R-R interval. Pulse interval is plotted against SBP and the slope of the regression line is calculated. Many sequences are taken over a period of time, and the average of the slope of all regression lines are used to quantify the BRS. Adapted from [25].

One of the advantages of the sequence technique is the separate identification of baroreceptor activation and deactivation.

2.2.1   Reliability of the Sequence Technique

Bertieneri and his colleagues found that there were high correlation coefficients between average estimates of BRS obtained with the traditional pharmacological iv injection of a vasoactive substance, and using the sequence technique [25]. The average BRS obtained from the sequence technique of sufficient duration (at least 10-15 minutes of recording) are highly reproducible [25]. Finally, the average BRS obtained by the sequence method largely represent the baroreflex, because the length of most sequences

doesn't exceed 6 beats, and because the sequences disappear following atropine injection [25].

2.2.2 Sequence Technique with Latency

Persson *et al.* (2001) [27] mentions the spontaneous latency of the baroreflex control of HR (and subsequently BP). To incorporate this delay parameter into the sequence technique, BRS can be calculated for a range of lags (L0,L1,L2,L3). A latency of 0, 1, 2 or 3 cardiac cycles can be calculated for positive or negative sequences. L0 refers to changes in PI and SBP for the same cardiac cycle, L1 for a change in SBP associated with a corresponding change in PI for the next beat, and similarly for L2 and L3. Figure 10 illustrates a sequence calculation for a cardiac cycle latency of 1 (L1):
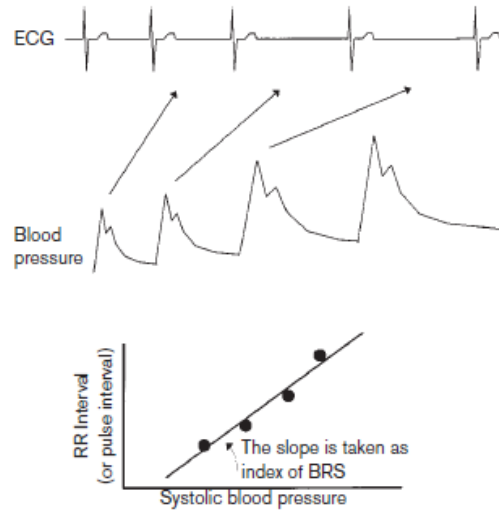
Figure 2.2: An illustration of how the sequence technique can be calculated for a lag of 1 cardiac cycle [27].

2.3   Measuring BRS in the Frequency Domain

BRS can be calculated in the frequency domain as well: SBP and HR changes can be quantified as a function of their respective frequencies, by taking the square root of the ratio between PI spectral powers and SBP spectral powers. The result is called the α-coefficient. The frequencies of interest in humans occur at 0.1 Hz (Low Frequency, LF) and at the frequencies of 0.2 - 0.3 Hz (High Frequency, HF). Pagani *et al.* (1988) describes the high frequency respiratory component to reflect parasympathetic vagal modulation, while the power of the low frequency has both sympathetic and parasympathetic influences. Reference [24] also confirms this, with efferent vagal activity (the vagus nerve being a major parasympathetic nerve) being a major contributor to the HF component of the frequency spectrum. This was confirmed by clinical and experimental observations through electrical vagal stimulation, muscarinic receptor blockade and vagotomy. Ongoing debate about the interpretation of the LF component exists, with some considering it as a marker of sympathetic modulation, and others considering it a marker of both sympathetic and parasympathetic influences. Figure 2.3 illustrates how to calculate the α_{HF} and α_{LF} -coefficients:
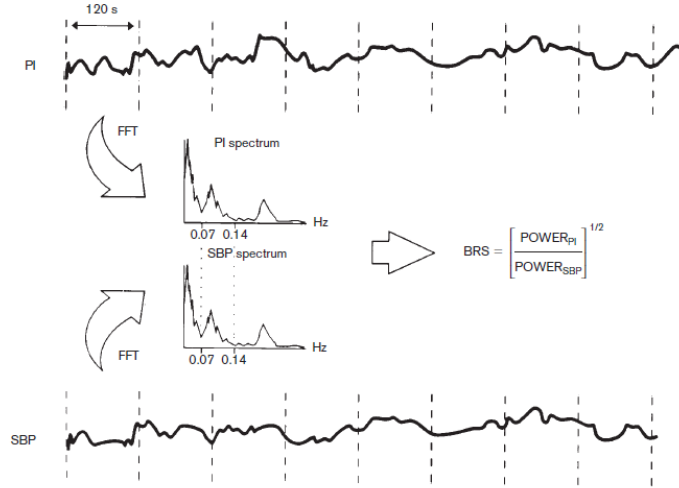
Figure 2.3: A schematic on how to find the BRS in the frequency domain [25], [28].

Due to the very nature of HRV, the RR interval and SBP time series signals are inherently unevenly sampled. The HRV signal is one example of a non-stationary signal, whose frequency constantly changes with time. Figure 2.4 illustrates this very fact. RR_1 and RR_2 are not of equal time duration and neither is PP_1 and PP_2. Hence, the HRV

signal (with RR interval plotted as a function of time) and SBP variability signal (with SBP plotted as a function of time) are unevenly sampled. We can use the term 'sample' because each RR interval and SBP corresponds to a discrete cardiac cycle or heart beat. One can also derive the HRV by plotting the RR interval or SBP as a function of cardiac cycle number. Because of this uneven sampling, one cannot just simply take a fourier transform (FT), as this assumes an even sampling rate. Several frequency spectrum techniques are investigated as outlined below.
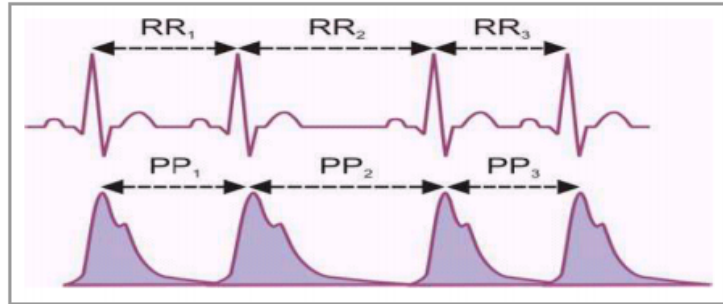
Figure 2.4: Illustration of the varying nature of HRV, RR_1, RR_2 & RR_3 will not be of equal time duration. Figure taken from [17].

2.3.1 Fast Fourier Transform

The commonly used fast fourier transform (FFT) algorithm developed by Cooley and Tukey in 1965 that is used to calculate the discrete fourier transform (DFT) of an evenly sampled signal.

The DFT is given by:

$$F[n] = \sum_{k=0}^{N-1} f[k]e^{-j\frac{2\pi}{N}nk} \quad for(n = 0 : N-1) \tag{2.1}$$

where:

N is the total number of samples

n and k are counting variables for discrete frequency & sample number

$f[k]$ is the kth sample of the signal

$F[n]$ is the nth calculated frequency bin of the signal f

To calculate this, we must first interpolate the signal so it is evenly sampled.

Using MATLAB's version *2015a* resample function, we can interpolate the signal with a desired sampling frequency *Fs*. MATLAB does this by using a polyphasic antialiasing filter to resample the signal at the specified *Fs* using an evenly spaced grid. The default linear interpolation method was used. The specified sampling frequency *Fs* had to be greater than twice the maximum HR, as per the nyquist sampling theorem.

Once the signal is evenly interpolated, the *FFT* command can be used to obtain the frequency spectrum of the signal. In this thesis, the *pwelch* command was used to obtain the power spectrum of the signal using the Welch periodogram. It uses a Hamming window function to break the signal into overlapping segments and takes the average of the FFT's that were calculated for each window. Using a window function reduces spectral leakage commonly associated with taking a sample set of data that may not have an integer number of periods.

2.3.2   Non-Uniform Discrete Fourier Transform (NDFT)

The concept of the NDFT was developed to deal with obtaining the frequency spectrum of unevenly sampled signals. Non stationary signals are ubiquitous in nature: many biological signals such as the ECG, time varying auditory signals and EEG signals are all considered non-stationary. The HRV is one such signal which falls into this category. Bagchi et al [29] defined the NDFT as follows:

$$X_{ndft}(m) = \sum_{n=0}^{N-1} x[n] z_m^{-n} \tag{2.2}$$

where:

N is the total number of samples

n is the sample number

$x[n]$ is the nth sample of the signal

$X(m)$ is the mth calculated frequency bin of the signal x

z_m is a distinct point located arbitrarily on the z-plane.

However, a more straightforward method of calculation comes from [30], [31]:

$$X_{ndft}(m) = \sum_{n=0}^{N-1} x[n] e^{-j\frac{2\pi}{T}mt_n} \tag{2.3}$$

where:

N is the total number of samples

n is the sample number

$x[n]$ is the nth sample of the signal

$X(m)$ is the mth calculated frequency bin of the signal x

t_n is the sample time

T is the total time

2.3.3 Lomb-Scargle Periodogram

The Lomb-Scargle periodogram (LSP) is a least mean squares regression method to estimate the power spectrum of a signal. The LS method is based on a least mean squares fit of sinusoids to data samples. The difference between the lomb-scargle method and the FFT is that a time offset is utilised in the LSP. The time offset guarantees the time invariance of the computed spectrum. Because of this, the samples need not be evenly sampled, with the LS periodogram given by the following equation:

$$P_{LS}(f) = \frac{1}{2\sigma^2} \left\{ \frac{[\sum_{k=1}^{N}(x_k - \bar{x})cos(2\pi f(t_k - \tau))]^2}{\sum_{k=1}^{N} cos^2(t_k - \tau)} + \frac{[\sum_{k=1}^{N}(x_k - \bar{x})sin(2\pi f(t_k - \tau))]^2}{\sum_{k=1}^{N} sin^2(t_k - \tau)} \right\} \tag{2.4}$$

where

$$\bar{x} = \frac{1}{N} \sum_{k=1}^{N} (x_k - \bar{x})^2 \tag{2.5}$$

$$\sigma^2 = \frac{1}{N-1} \sum_{k=1}^{N} (x_k - \bar{x})^2 \tag{2.6}$$

and

$$tan(2(2\pi f)\tau) = \frac{\sum_{k=1}^{N} sin(2(2\pi f)\tau_k)}{\sum_{k=1}^{N} cos(2(2\pi f)\tau_k)} \tag{2.7}$$

Equations 2.5 and 2.6 are respectively the mean and variance of the data, while equation 2.7 is the time offset.

2.4   Measuring HRV in the Frequency Domain

Measuring HRV in the frequency domain involves taking the frequency spectrum of the HRV signal and measuring the respective powers in the low and high frequency bands, and was illustrated in table 2.2. This entails using any of the frequency spectrum estimation techniques found in section 2.3.1, 2.3.2 and 2.3.3.

2.5   Measuring Power: Parseval's Theorem

Both HRV and BRS frequency analysis techniques involve finding the power in specific frequency bands. This can be done by integrating the area under the bands, or by taking advantage of Parseval's theorem, which simply states the power of a signal in the time domain is equal to the power of the signal in the frequency domain. Parseval's theorem can be expressed in the following form:

$$\sum_{n=0}^{N-1} x^2[n] = \frac{1}{N} \sum_{m=0}^{N-1} |X[m]|^2 \tag{2.8}$$

When measuring band power, it is easier to work with normalised units (n.u) rather than absolute powers. Table 2.2 illustrates how to calculate n.u values. Very low frequency (VLF) is subtracted because we are only interested in the controlled and balanced behaviour of the two branches of the autonomic nervous system. VLF values are due to other factors such as hormonal and thermoregulation of HRV, and even the validity of this has come into question. In any case, VLF values are of little interest when considering the autonomic regulation of HRV.

2.6 Time Frequency Response

Another way to visualise HRV is to obtain a time-frequency plot of the HRV spectrum. This shows us information regarding the variation of frequency with regards to time, and can show us beat to beat variability and long term heart rate drift.

The time-frequency response is shown through a spectrogram, which utilises the short term fourier transform (STFT) to window the data and calculate the fourier transform over time. The value or visual intensity of the power is given as a function of time and frequency and can be seen on the spectrogram. The STFT can be expressed in the following form:

$$X[k,n_0] = \sum_{n=0}^{N_{FT}-1} x[n_0+n].w[n].e^{-j\frac{2\pi kn}{N_{FT}}} \tag{2.9}$$

where:

k is the frequency index

n_0 is the time index

$x[n]$ is the nth sample of the signal

$w[n]$ is the window used

$e^{-j\frac{2\pi kn}{N_{FT}}}$ is the DFT kernel

2.6.1 Time Frequency Resolution

Time frequency-resolution refers to the trade off between frequency resolution and time resolution. Having higher resolution in one quantity leads to poorer resolution in the other. This is because frequency and time resolution are inversely proportional due to Heisenberg's uncertainty principle. If we want finer time resolution, smaller windows should be taken which will give poorer frequency resolution.

Chapter 3

SHR and WKY Rats with and without Carotid Field Stimulation

3.1 Experimental Outline and Analysis Method

BRS and HRV was investigated between carotid field stimulated and non-stimulated normotensive WKY (control group, n = 3) and SHR rats(hypertensive, n = 2) using the time based sequence technique, NDFT, FFT (welch periodogram) and the Lomb-Scargle periodogram. The rats were stimulated for blocks of time at 100 Hz. Data was extracted from Spike (v7.16) using custom made R scripts prepared by Dr. Mark Butlin (Faculty of Medicine and Health Sciences, Macquarie University). BRS was compared between the control and hypertensive group. BRS was also compared between the different time and frequency domain techniques to see if they gave similar results. It is to be noted that in all these rats, no period of analysis exceeded 10 minutes of data.

Stimulation of the carotid complex causes noise corruption to the ECG signal, which renders it unusable. One method is to take the 2nd derivative of the blood pressure waveform which results in a waveform similar in shape to the ECG. The ECG and blood pressure waveform are in temporal sync and hence, the differentiated BP waveform was used to extract the RR interval for analysis. Figures 3.1 and 3.2 below illustrates:
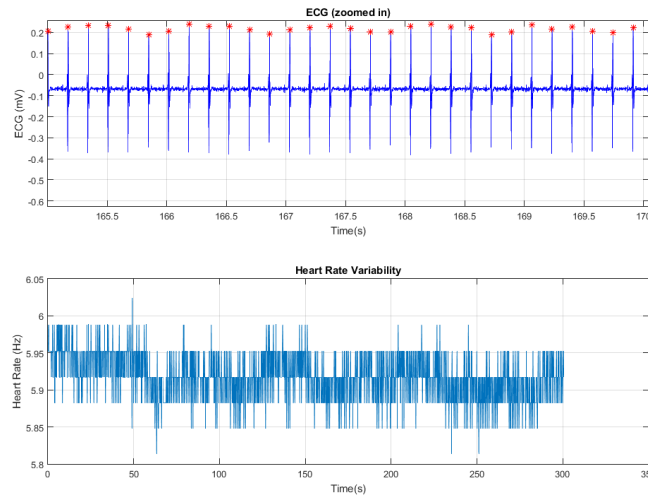
Figure 3.1: ECG with derived HRV signal, with the bottom y-axis converted to Hz (both plots are from the same rat.)
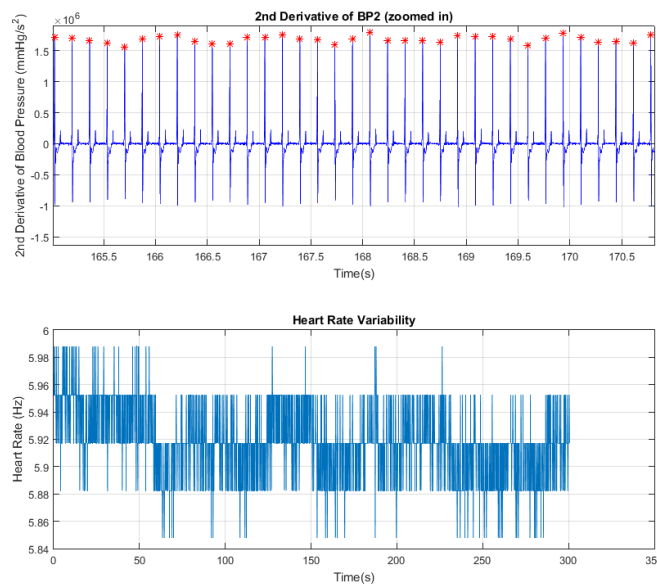
Figure 3.2: 2nd differential of blood pressure with derived HRV signal (both plots are from the same rat.). The DC offset was taken out, hence the graph goes through 0 in the top graph. The y-axis of the bottom graph has been converted to Hz. We can see the effects of breathing in both the ECG and 2nd derivative of the blood pressure waveform; this is commonly seen in rat data. The modulation of intrathoracic pressure in the breathing cycle leads to changes in venous return, which leads to modulation of blood pressure with the breathing cycle. Subsequent heart rate changes occur due to baroreceptor feedback from the blood pressure changes in the breathing cycle.

A frequency histogram was generated in R for both stimulated and non-stimulated in SHR and WKY. Figures 3.3 and 3.4 below illustrates for a typical SHR and WKY rat respectively. Stimulated normotensive rats show a marked skewness in the shape of the histogram compared to the hypertensive rats. This is a novel observation that has not yet been reported in literature.
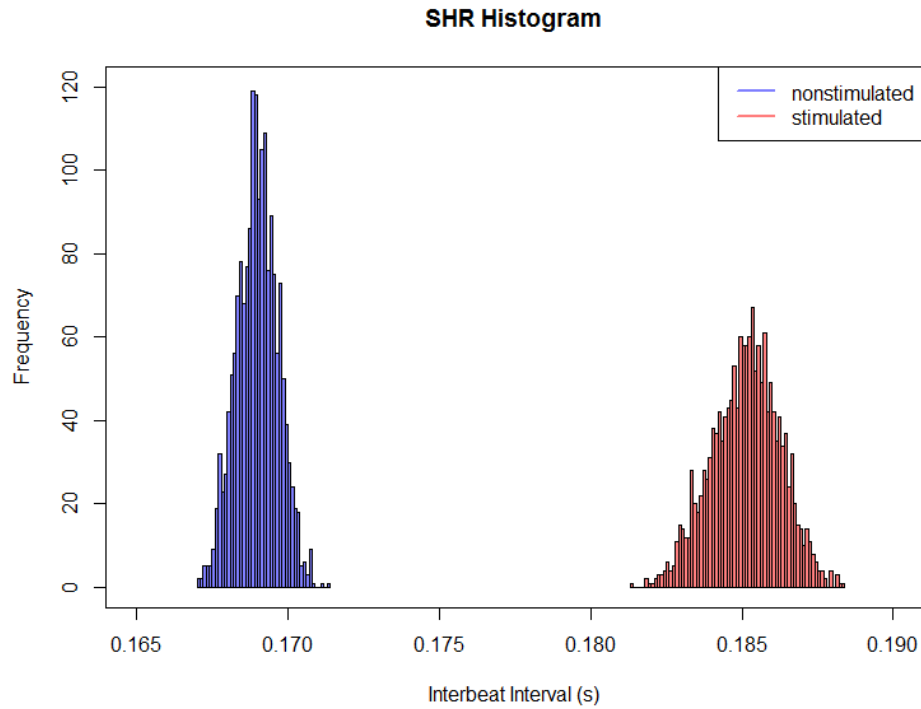
Figure 3.3: Histogram showing RR intervals for a single stimulated and non-stimulated SHR rat
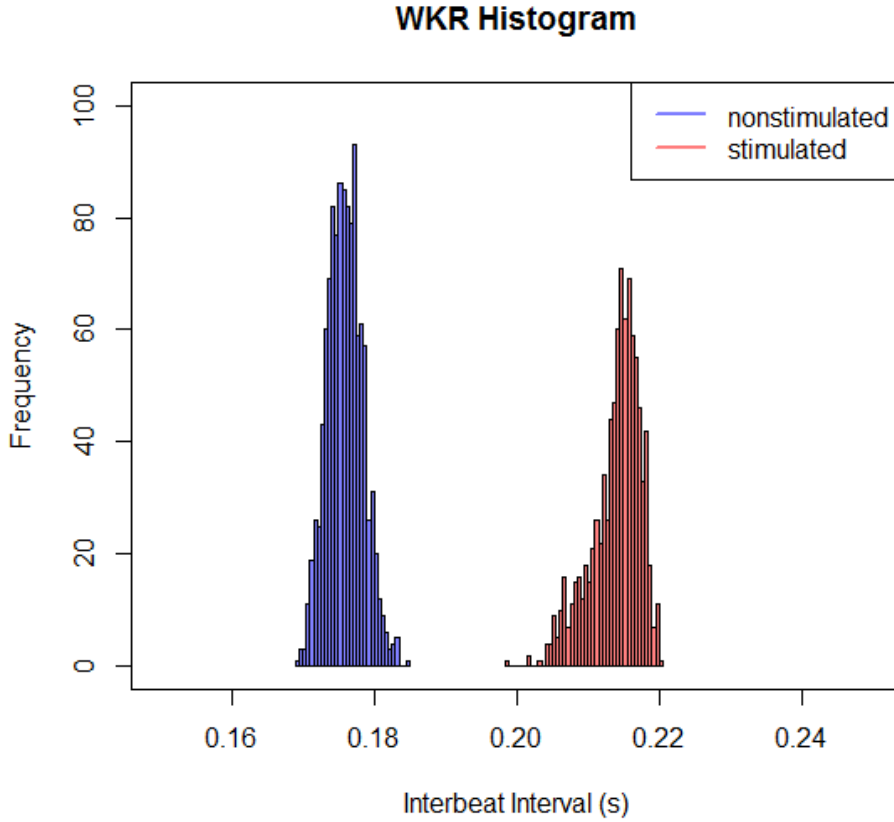
Figure 3.4: Histogram showing RR intervals for a single stimulated and non-stimulated WKY rat

3.2 Results

Results of HRV and BRS quantification are presented in the following sections.

3.2.1 BRS: Time Domain

The sequence technique was applied with a threshold systolic pressure of 1 mmHg and R-R interval of 1 ms with lags of 0, 1, 2 and 3 cardiac cycles between detected systolic blood pressure sequences and R-R interval sequences using custom made MATLAB scripts (see appendix). These thresholds were chosen because it gave the maximum total number sequences for each rat.

Figure 3.5 shows typical sequences for a single non-stimulated WKY rat (BRS is given in units of ms/mmHg):
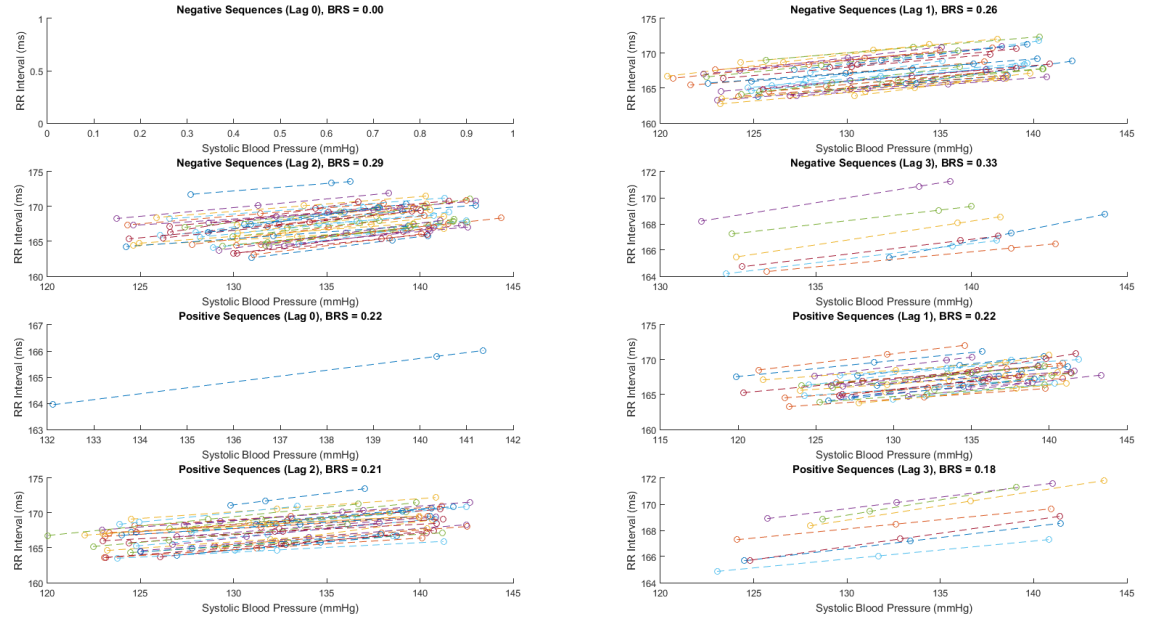
Figure 3.5: Illustration of sequences with lags of 0, 1, 2 and 3 cardiac cycles between detected systolic blood pressure sequences and R-R interval in non-stimulated WKY. No sequences were detected for negative sequences (lag 0). A lag 0 assumes that the heart rate change is instantaneous with a change in blood pressure.

The average BRS was calculated for each rat:

Table 3.1: Average BRS for each rat

Sequence Technique BRS	(units of ms/mmHg)			
	WKY	WKY Stim	SHR	SHR Stim
rat 1	0.32	0.43	0.20	0.24
rat 2	0.41	1.07	0.69	0.30
rat 3	0.25	0.61	-	-
average BRS	0.33	0.70	0.45	0.27
S.D	0.08	0.33	0.35	0.04

We can see from table 3.1 that for SHR rats, stimulation causes an increase in BRS in one rat and a decrease in the other rat. Averaging these two opposite values loses the individual trend information. With such a small sample size of only two rats, it is important to look at the BRS of individual rats.

An unpaired two tailed t-test was applied to the groups indicated in table 3.2 to see if any statistical significance existed between rat strain. There was no statistically significant difference found between the respective groups. A paired two-tailed t-test was applied to stimulation/not-stimulated rats of the same strain. It was found there was no significant difference in BRS in stimulated and non-stimulated WKY and SHR rats (tables 3.3 & 3.4).

Table 3.2: p-value for select groups

	Groups		
	WKY / WKY stim	SHR/SHR stim	SHR/WKY
p-value	0.14	0.57	0.71

Table 3.3: Statistical significance between number of sequences in stimulated/ nonstimulated SHR rats, using a paired t-test

	Number of sequences	
SHR	stimulated	not stimulated
rat 1	155	94
rat 2	26	1
p-value	**0.25**	

Table 3.4: Statistical significance between number of sequences in stimulated/ non-stimulated WKY rats, using a paired t-test

	Number of sequences	
WKY	Stimulated	Not Stimulated
rat 1	39	36
rat 2	84	336
rat 3	19	159
p-value	**0.22**	

3.2.2   BRS: Frequency Domain

The NDFT, LSP and Welch periodograms were used to obtain the frequency spectrum of the HRV signal.

Snippets of MATLAB code are given below:

NDFT:

```matlab
for k = 0:L-1
    for n = 0:L-1
        P(k+1) = P(k+1) + ...
            RR_Interval(n+1)*exp((-1i*2*pi*time_seconds(n+1)*k/T));
    end
end
```

Resampling + Welch periodogram:

```matlab
[Y,Ty] =resample(RR_Interval,time_seconds,fs); % Y is resampled ...
    RR_interval
[pxx,f] = pwelch(Y,512,128,512,fs,'power');
```

Lomb-Scargle Periodogram:

```matlab
plomb(RR_Interval,time_seconds,'Pd',[0.99, 0.5]);
```

The time frequency spectrogram was obtained via the following function:

```matlab
spectrogram(Y,256,250,256,fs,'yaxis')
```

Figure 3.6 illustrates the various HRV frequency spectra for an SHR stimulated rat:
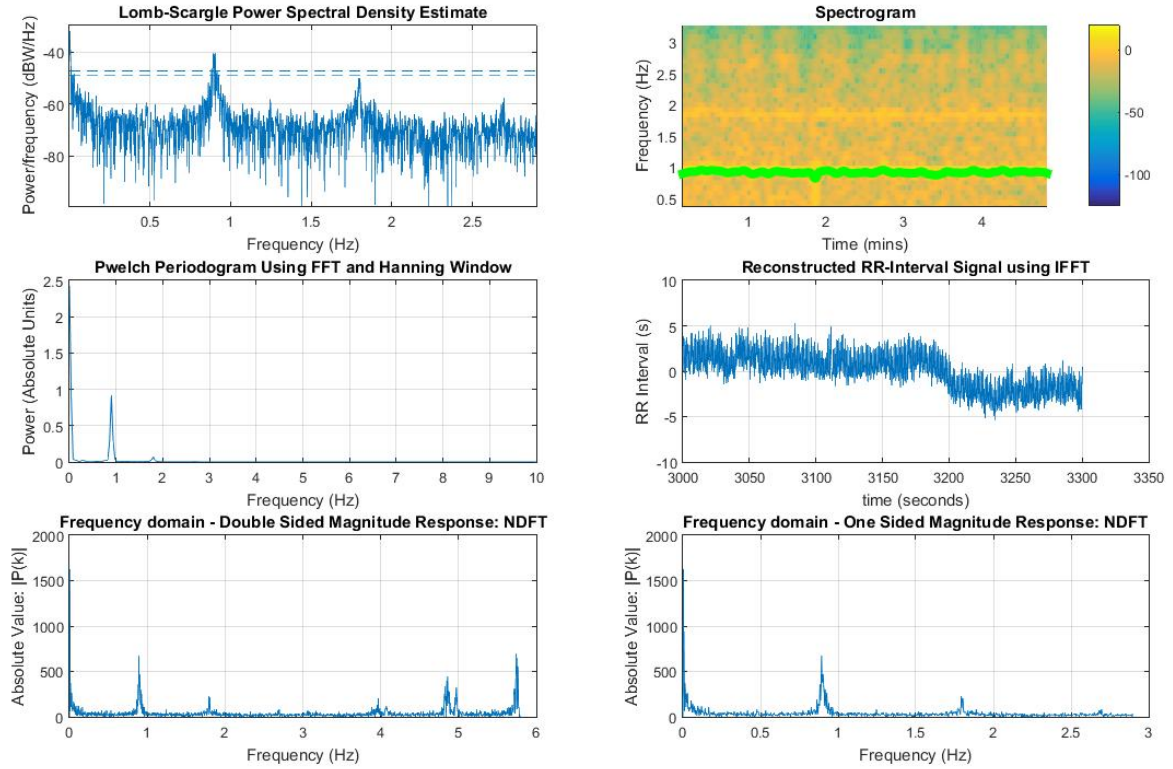
Figure 3.6: frequency spectra for the SHR rat using various techniques. The reconstructed RR-interval signal was obtained using MATLAB's ifft function.

Figure 3.7 illustrates the various systolic blood pressure frequency spectra for an SHR stimulated rat.
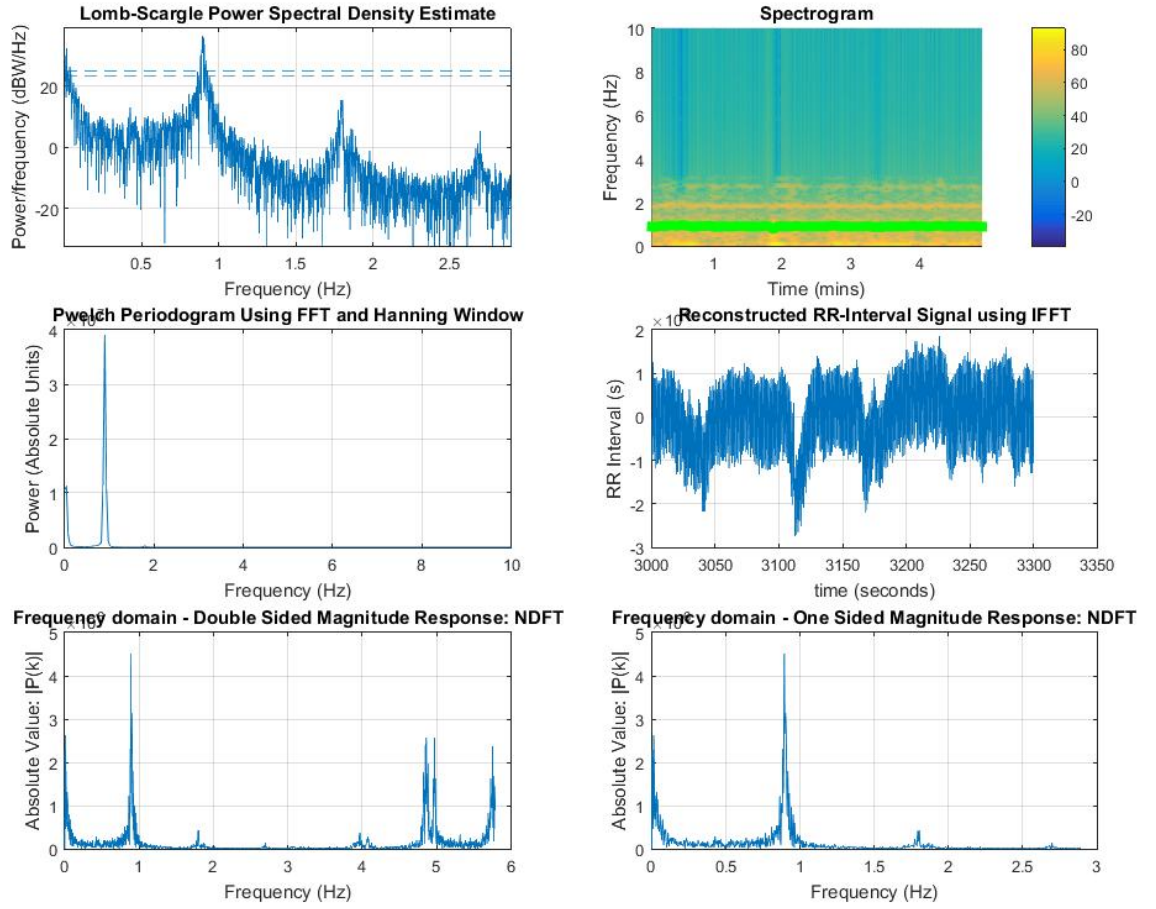
Figure 3.7: SBP frequency spectra for the SHR rat using various techniques. The reconstructed signal was obtained using MATLAB's ifft function. The highest amplitude in the low frequency band in the spectrogram was tracked with a solid green line.

It was found that there were no significant difference in BRS values between the sequence technique and the 3 frequency techniques (NDFT, LSP and FFT welch periodogram). The average BRS values and their standard deviations were compared between the various techniques between the LF and HF alpha-coefficients in figures 3.8 and 3.9:
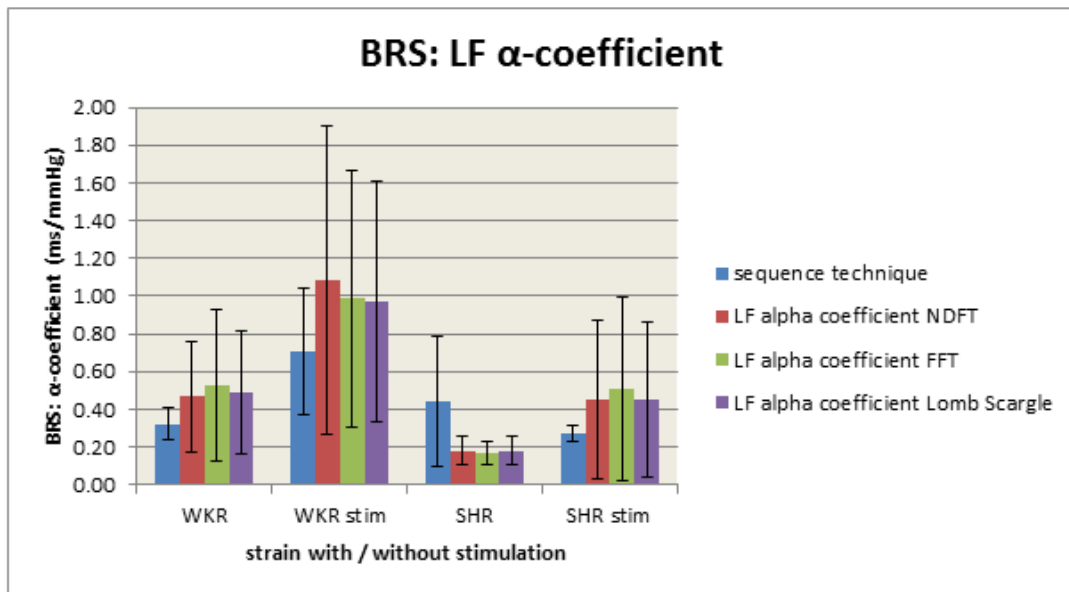
Figure 3.8: Comparison of BRS values with the LF alpha coefficient calculated from time and frequency different techniques
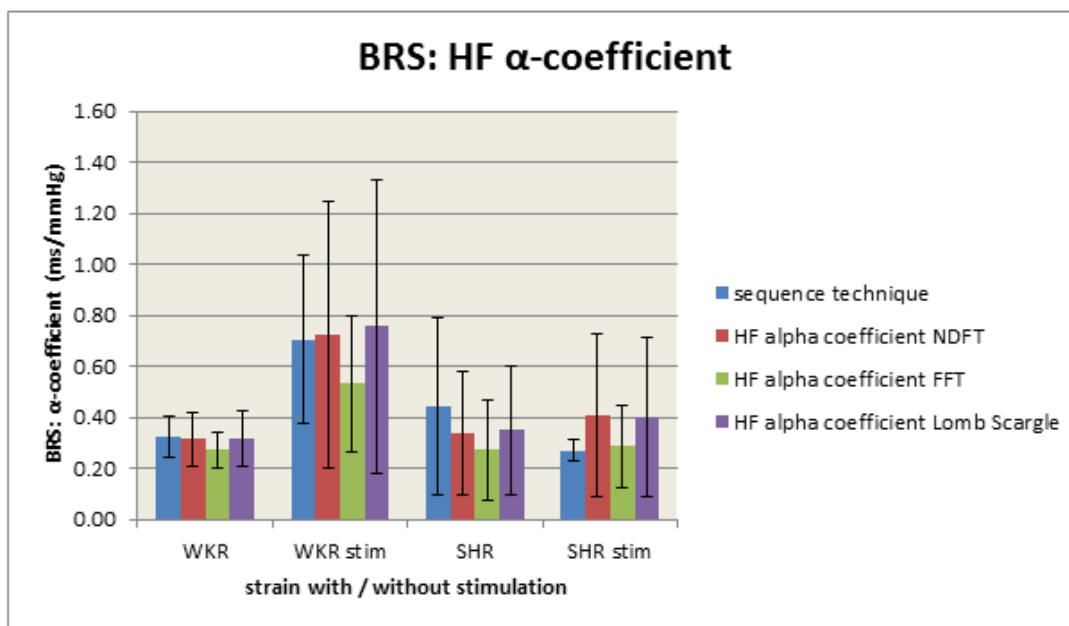
Figure 3.9: Comparison of BRS values with the HF alpha coefficient calculated from time and frequency techniques

3.2.3   HRV: Time Domain

HRV was measured using the SDNN interval, figure 3.10 illustrates:
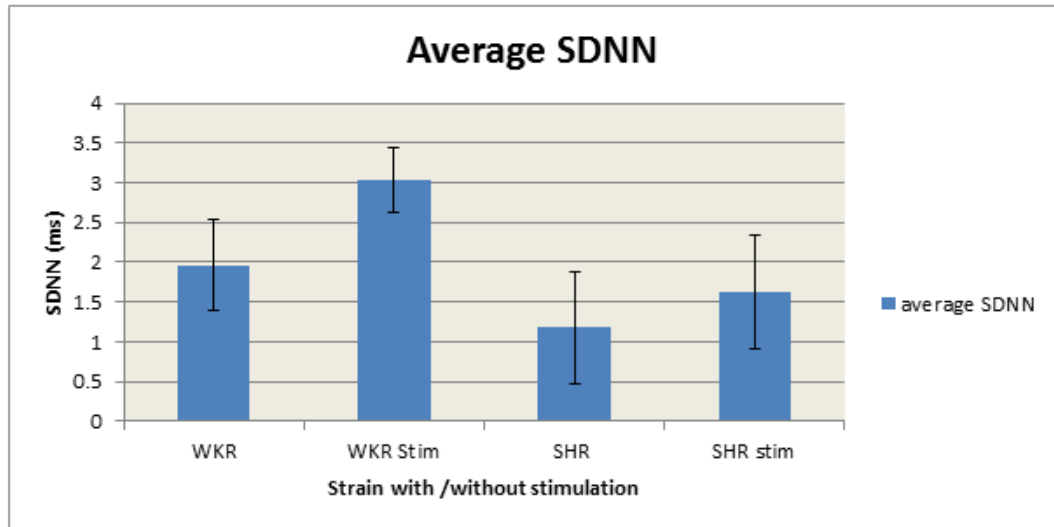
Figure 3.10: Average of SDNN for stimulated and non-stimulated SHR / WKY

3.2.4 HRV: Frequency Domain

HF and LF were compared for each frequency technique to the time domain sequence technique.
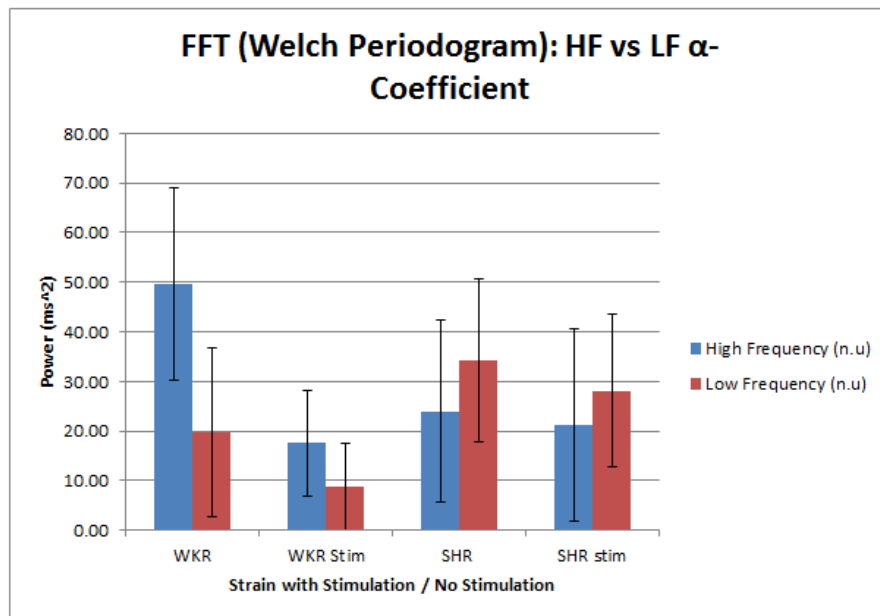
Figure 3.11: FFT HF & LF calculations for each stimulated / non-stimulated strain $\pm$ standard deviation
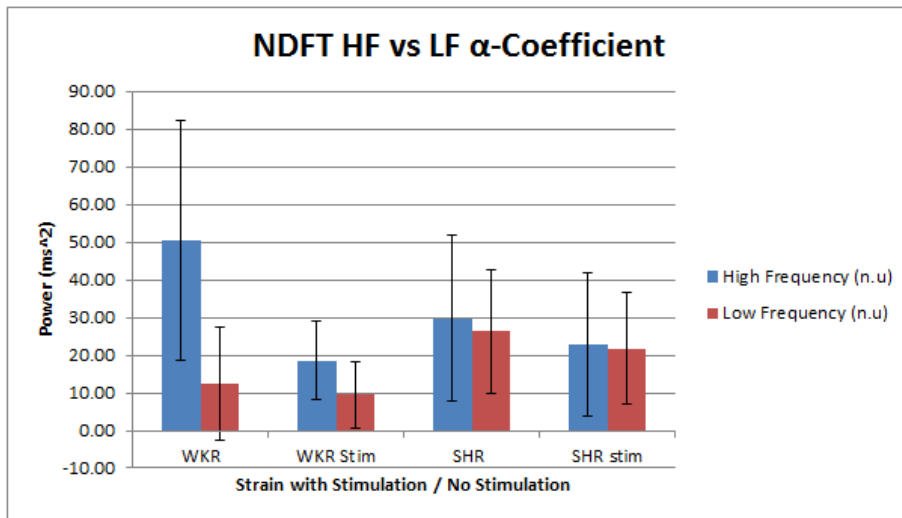
Figure 3.12: NDFT HF & LF calculations for each stimulated / non-stimulated strain ± standard deviation
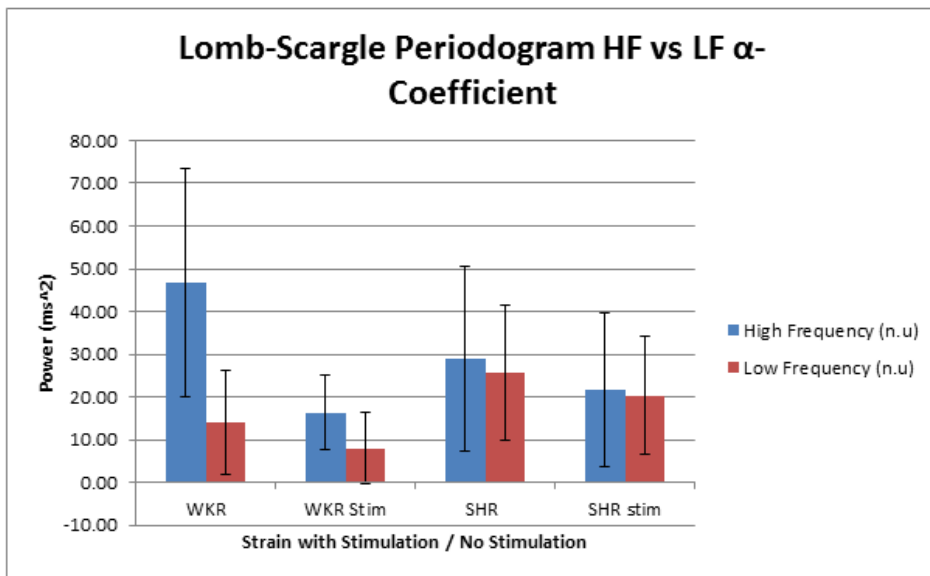
Figure 3.13: LSP HF & LF calculations for each stimulated / non-stimulated strain ± standard deviation

3.3   Discussion

Figures 3.1 and 3.2 show that for both ECG and 2nd derivative of the blood pressure waveform, the HR varies from 5.8 to 6 Hz for both quantities. These two HRV graphs are quite similar, and for analytical consistency, this method was used regardless

of stimulation for both SHR and WKY.

The histograms in figures 3.3 and 3.4 illustrate an important concept behind carotid stimulation: field stimulating the baroreceptor complex causes increased neural firing of the nerve from the baroreceptors which causes an immediate negative feedback response through the baroreflex. The baroreflex slows down the HR by increasing the RR interval through parasympathetic stimulation and sympathetic inhibition. One of the ways the body tries to reduce blood pressure is to reduce cardiac output (CO).

Since CO = HR × SV, decreasing HR causes a decrease in CO. If there is a decrease in CO, less blood is ejected from the heart with each cardiac cycle, there will be less blood pressure against the vessel walls and hence blood pressure becomes lower. Also, blood volume affects end diastolic volume and consequently stroke volume. With decreased stroke volume, there is decrease in venous return, causing a decrease in cardiac output and hence, a decrease in blood pressure.

3.3.1 BRS in the Time Domain

BRS was calculated using the time based sequence technique. Average BRS was calculated by averaging the BRS for every detectable lag, positive and negative (the latter mentioned BRS was calculated by averaging the BRS for each sequence detected in the lag). Table 3.1 indicates that average BRS increased for stimulated WKY rats compared with non-stimulated, and that average BRS decreased for stimulated SHR rats compared with non stimulated SHR. The p-values in table 3.2 indicate there was no significant difference between the strains, and no difference between stimulated and non-stimulated strains. Table 3.3 shows that no significant difference was seen in the number of sequences detected in stimulated and non-stimulated SHR rats. Table 3.4 shows that no significant difference was seen in the number of sequences detected in stimulated and non-stimulated WKY rats.

SHR Rats

These results seem to suggest that there is no correlation whatsoever between stimulated and non-stimulated SHR, but one needs to look at the amount of data that was analysed to get a true picture. 2 rats are the absolute minimum amount to perform any statistical test, and hence, we can conclude that a sufficient sample size was not used

to perform any meaningful statistical tests, and the test was underpowered. The more sample data we have, the more representative the average and standard deviation will be of the whole population. Using the S.D measurements in table 3.1, we can calculate an appropriate sample size. Using [32], an appropriate sample size for WKY (stim and non stimulated) would be 5 rats, and 24 rats for SHR (stim and non-stimulated). We can however, look qualitatively at the number of sequences detected and see that stimulation increased the number of sequences detected in both rats compared with the non-stimulated strain. One plausible explanation for is that SHR are a hypertensive strain and have a dampened baroreflex, with poor short term regulation of blood pressure. Carotid field stimulation increases the nerve firing from the baroreceptors which gives rise to the negative feedback mechanism that is the baroreflex. Since the baroreflex is more active due to neural stimulation than before stimulation, more *spontaneous sequences* of increasing / decreasing blood pressure are detected, with a concomitant increase / decrease in RR interval (decrease and increase in HR respectively).

WKY Rats

The same problems arise in when looking at the t-tests results for stimulated / non-stimulated WKY rats. The test is underpowered, with only 3 WKY rats, and is not a sufficient sample size to discern any meaningful results. We can also look quantitatively at the number of sequences detected in stimulated/ non-stimulated WKY rats. WKY rats can regulate their blood pressure without the need for carotid stimulation, however, we can see a general trend of reduced sequences during stimulation. The baseline of blood pressure is reduced during stimulation, so it is possible that the baroreceptor that is being stimulated is saturated and no longer able to effectively regulate blood pressure through the baroreflex. Sequences are still detected by the other carotid baroreceptor and the aortic arch. Because the baseline arterial blood pressure has been reduced from its previous higher set point, the baroreceptors try to raise the blood pressure, which involves sympathetic stimulation and parasympathetic inhibition. Sympathetic stimulation takes longer to act than parasympathetic stimulation, which is why less sequences are detected with the MATLAB script, as it only calculates up to lag 3, with 1 mmHg and 1ms as thresholds.

An important point to note is that these results are contrary to the results by Kouchaki

et al [1] who found that stimulation did not affect the acute baroreceptor function peak gain. In that experiment, a bolus of the vasoconstrictor phenylephrenine was administered, initially causing a large change in MAP. As the effects of phenyephrenine wore off, MAP and HR came back to their normal response. Due to the fact that BRS was measured over a very large pressure range, the gradient of the inflexion point of the HR vs MAP curve in figure 1.10 was taken to be the BRS. In this study of quantifying BRS using the sequence technique, our pressure thresholds are only 1 mmHg, and hence, when BRS is calculated, it is only taking into account a small portion of the curve generated by using pharmacological methods. The problem with this is, we do not know where on the curve BRS is calculated, and can change arbitrarily depending on the tangent of the curve at that point. This is an important pitfall of using the sequence technique, and must be taken into account when using it.

3.3.2   HRV in the Time Domain

From figure 3.10, HRV is more variable in WKY strains compared to the SHR strain due to a larger spread of values in RR intervals from the average. This is expected, as WKY have a working baroreflex and can regulate their short term blood pressure via the constant regulatory balance of the sympathetic and parasympathetic nervous systems. SHR have a dampened baroreflex and lack the negative feedback to vary their heart rate accordingly. The HRV in stimulated WKY rats are larger than the non-stimulated WKY possibly due to the negative feedback of the baroreflex being actively engaged by baroreceptors in the non-stimulated carotid artery and the aortic arch. We know that carotid field stimulation causes the baseline of MAP to drop, and the baroreflex tries to maintain arterial pressure at the previous non-stimulated set point.

3.4   BRS in the Frequency Domain

Figure 3.6 shows an example of the various frequency domain techniques used to find the autonomic components of HRV. The top left uses the Lomb-Scargle periodogram, which shows two distinct peaks at 0.95 Hz and 1.8 Hz. The same is show for the middle left welch periodogram where a smaller peak is discernible at 1.8 Hz. The NDFT is more interesting, where the two sided frequency spectrum (bottom left) are not exactly

symmetric in nature. This is probably due to the uneven nature of the data, and the fact that a window function was not used. The bottom right figure shows the one sided magnitude response by taking the left hand part of the NDFT graph. In all cases for WKY, stimulated WKY, SHR and SHR stimulated, the peaks matched in all 3 frequency techniques. One very important point of note is the low frequency component and the respiratory frequency of a rat. The typical breathing rate of a rat is about 85 breaths per minute (1.4 Hz). The approximate low frequency parasympathetic & sympathetic component falls anywhere from 0.2 - 1 Hz or higher. Hence, it is possible both physiological effects will affect the same part of the frequency spectrum; there will be 'mixing' of both spectra in the same region. The highest amplitude in the low frequency region was tracked with a thick bright green line and is presented below zoomed in:
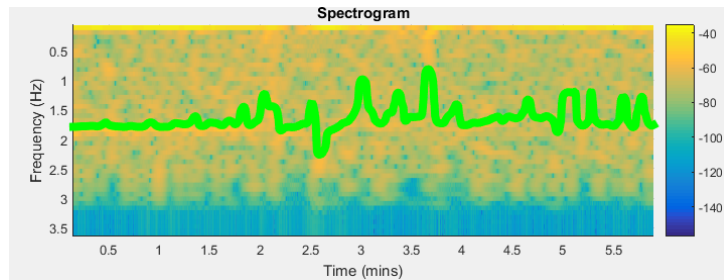
Figure 3.14: Zoomed in spectrogram showing frequency vs time.

Due to the oscillatory component of this line, it is most likely the respiratory frequency that is being tracked, since the rat is a free breathing animal while it is anaesthetised.

Another interesting phenomenon is the concept of allometry, where certain physiological parameters scale with animal size by a log factor. One example of this is that respiratory and heart rate, which gets higher in smaller animals. For example, humans have a heart rate of 60 bpm, rats with heart rate 300 bpm, mice with a heart rate 0f 600 bpm. The respiratory rate in humans is about 12-20 breaths per minute in a healthy adult. As there is a 5 fold increase in heart rate from humans to rats, there is an approximate 5 fold increase in respiratory rate.

Figures 3.8 and 3.9 present an interesting picture of the workings of the parasympathetic and sympathetic nervous systems. During stimulation, the LF & HF α-coefficients are increased in WKY rats. This is probably due to the fact that the system is trying to correct itself to the previous non-stimulated set point. During stimulation, there is barely any change in the HF α-coefficient, while there is an increase in the LF coefficient. This

could be due to sympathetic stimulation to increase HR to the previous set point.

3.5   HRV in the Frequency Domain

Figures 3.11, 3.13 and 3.12 show the relative powers of LF (defined in this dissertation as 0.2 -1 Hz) and HF(defined in this dissertation as 1-3 Hz) bands in stimulated and non-stimulated WKY and SHR strains. There have been some studies showing that the LF / HF ratio represents the sympatho-vagal balance. This has caused some controversy, as Milicivec et al (2013) [33] and [34] have stated vehemently that the LF/HF ratio does not accurately measure cardiac sympatho-vagal balance. In particular, Milicevic states the following reasons that the LF/HF ratio is not a reliable measure of sympatho-vagal balance:

- the complex nature of LF power has a poor relationship to sympathetic nerve activity

- non-linear interactions between sympathetic and parasympathetic nerve activity that are confounded by the mechanical effects of respiration and HR

Due to these reasons, it makes it impossible to delineate the physiological basis for LF/HF with any certainty. One way of quantifying HRV is by taking the time-frequency spectrum of the whole ECG waveform. Figure 3.15 illustrates this.
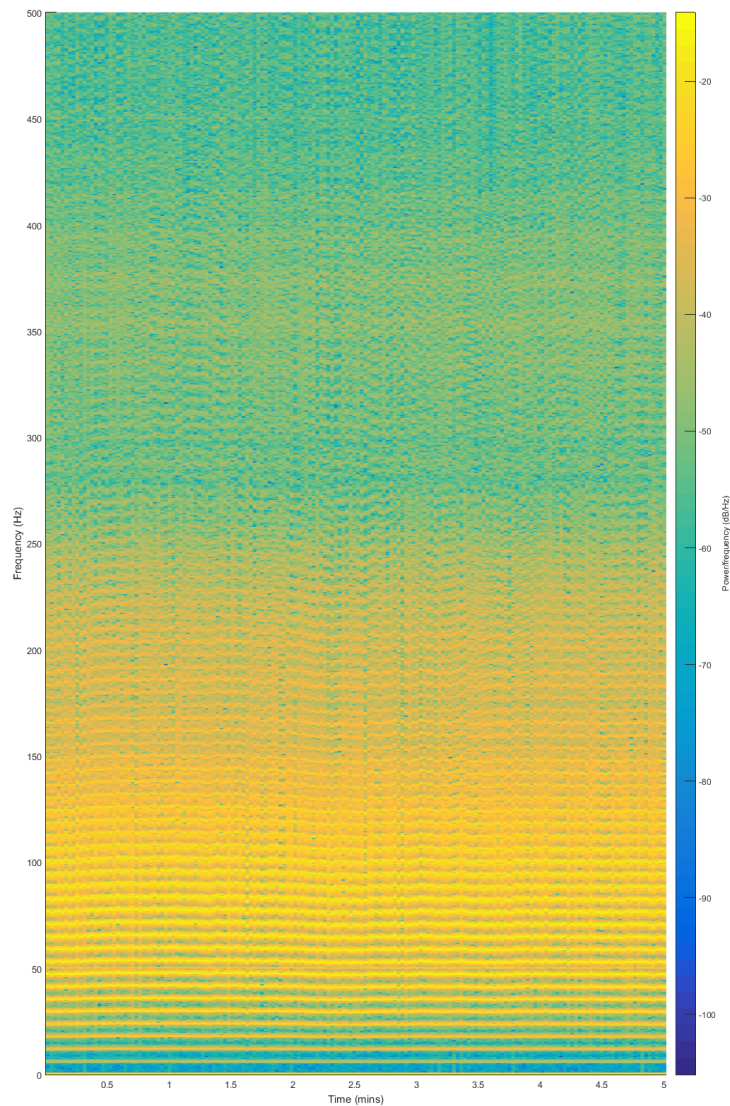
Figure 3.15: Spectrogram of full ECG waveform showing frequency vs time.

The temporal variation in HR and can be seen in the higher harmonics and can be tracked to see how HR varies with time. Of course, this doesn't give you any information of the autonomic nervous system control of HR.

Chapter 4

BRS and HRV Investigation in Diabetic and Wistar Rats

4.1 Experimental Outline and Analysis Method

HRV and BRS analysis of diabetic / control rats of the following experiment are presented in this section. Male, Wistar rats (6 weeks) were divide into control (n=8) and induced diabetes (intraperitoneal streptozotocin, 50 mg/kg, confirmed by blood glucose measurement, n=10). At 18 weeks, rats were anaesthetized (urethane, 1.3 g/kg) and an electrocardiogram and aortic blood pressure measured (1.2 F solid-state pressure tipped catheter, introduced via the femoral artery). BRS and HRV were compared using the time based sequence technique, NDFT, FFT (welch periodogram) and the Lomb-Scargle periodogram. Data was extracted from Spike (v7.16) using custom made R scripts prepared by Dr. Mark Butlin (Faculty of Medicine and Health Sciences, Macquarie University). BRS was compared between the control and hypertensive group. BRS was also compared between the different time and frequency domain techniques to see if they gave similar results. It is to be noted that in all these rats, no period of analysis exceeded 15 minutes of data.

4.1.1 BRS: Time Domain

The sequence technique was applied with a threshold systolic pressure of 1 mmHg and R-R interval of 1 ms with lags of 0, 1, 2 and 3 cardiac cycles between detected systolic

blood pressure sequences and R-R interval sequences using custom made MATLAB scripts (see appendix). Figure 4.1 shows typical sequences for a single Wistar rat (BRS is given in units of ms/mmHg):
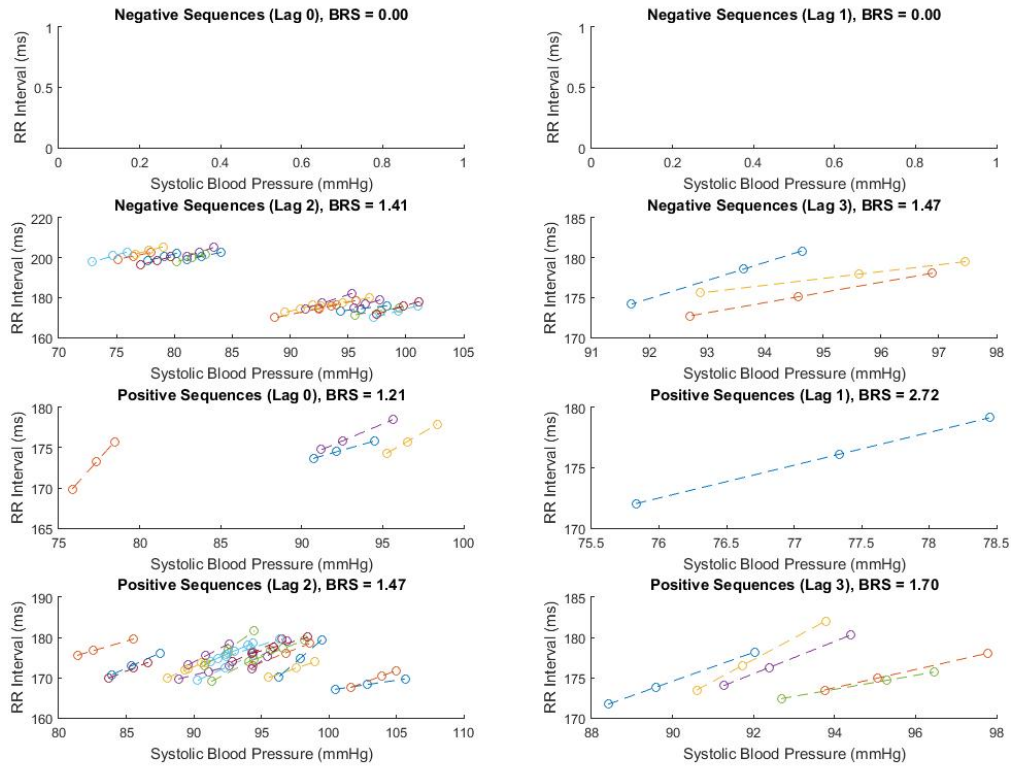
Figure 4.1: Illustration of sequences with lags of 0, 1, 2 and 3 cardiac cycles between detected systolic blood pressure sequences and R-R interval in a male Wistar rat. No negative sequences were detected for a lag of 0 and 1.

An unpaired two tailed student t-test showed a significant difference between the BRS in diabetic and control groups using the sequence technique (table 4.1).

Table 4.1: Average BRS calculated for each rat using the sequence technique. The calculation of average BRS was explained in section 3.3.1.

Sequence Technique	Control	Diabetic
rat 1	1.66	1.17
rat 2	0.74	0.82
rat 3	0.80	0.98
rat 4	0.81	1.83
rat 5	0.28	1.70
rat 6	1.10	1.07
rat 7	0.77	1.43
rat 8	0.94	1.27
rat 9		0.83
rat 10		1.53
p-value		**0.049**

4.1.2   BRS: Frequency Domain

The NDFT, LSP and welch periodograms were used to obtain the frequency spectrum of the HRV and systolic blood pressure variability signal, illustrated in figure 4.2 and 4.3:
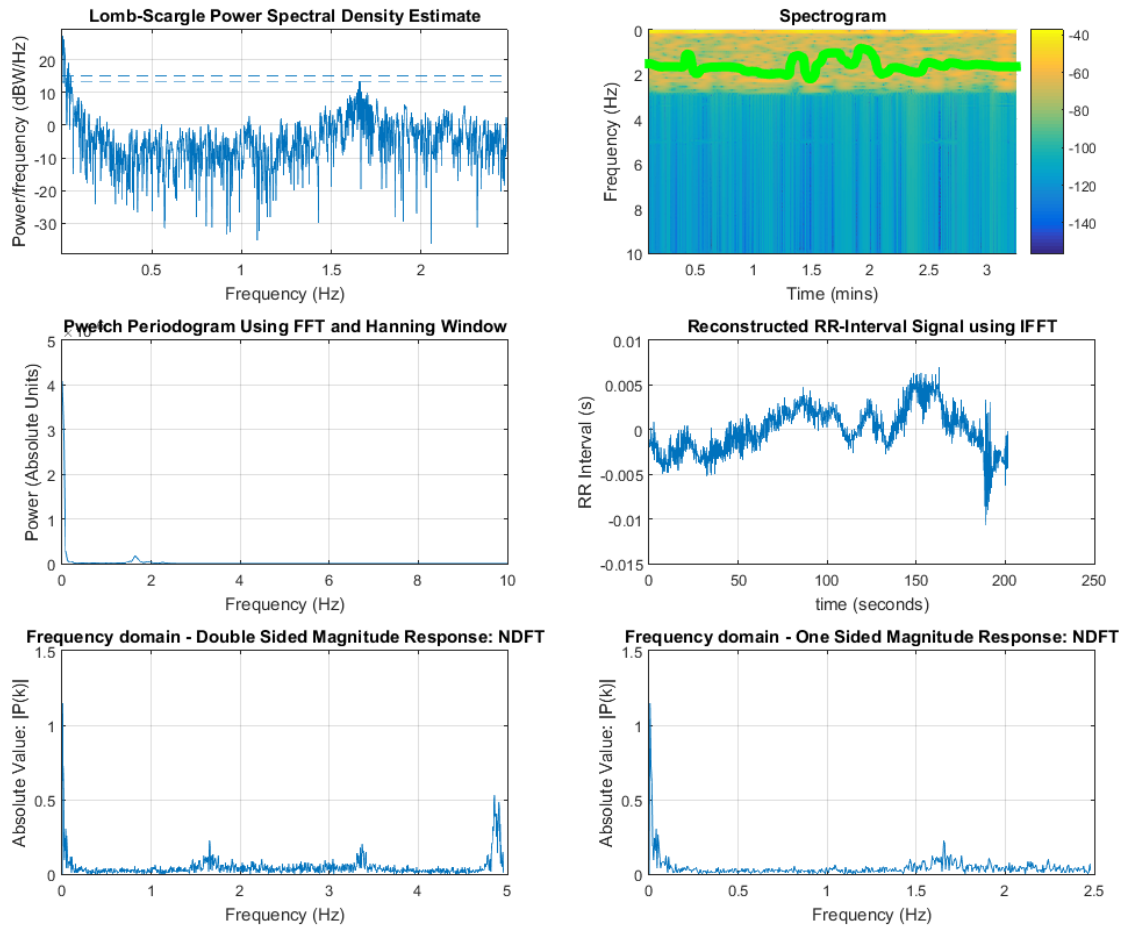
Figure 4.2: HRV spectrum for a diabetic rat
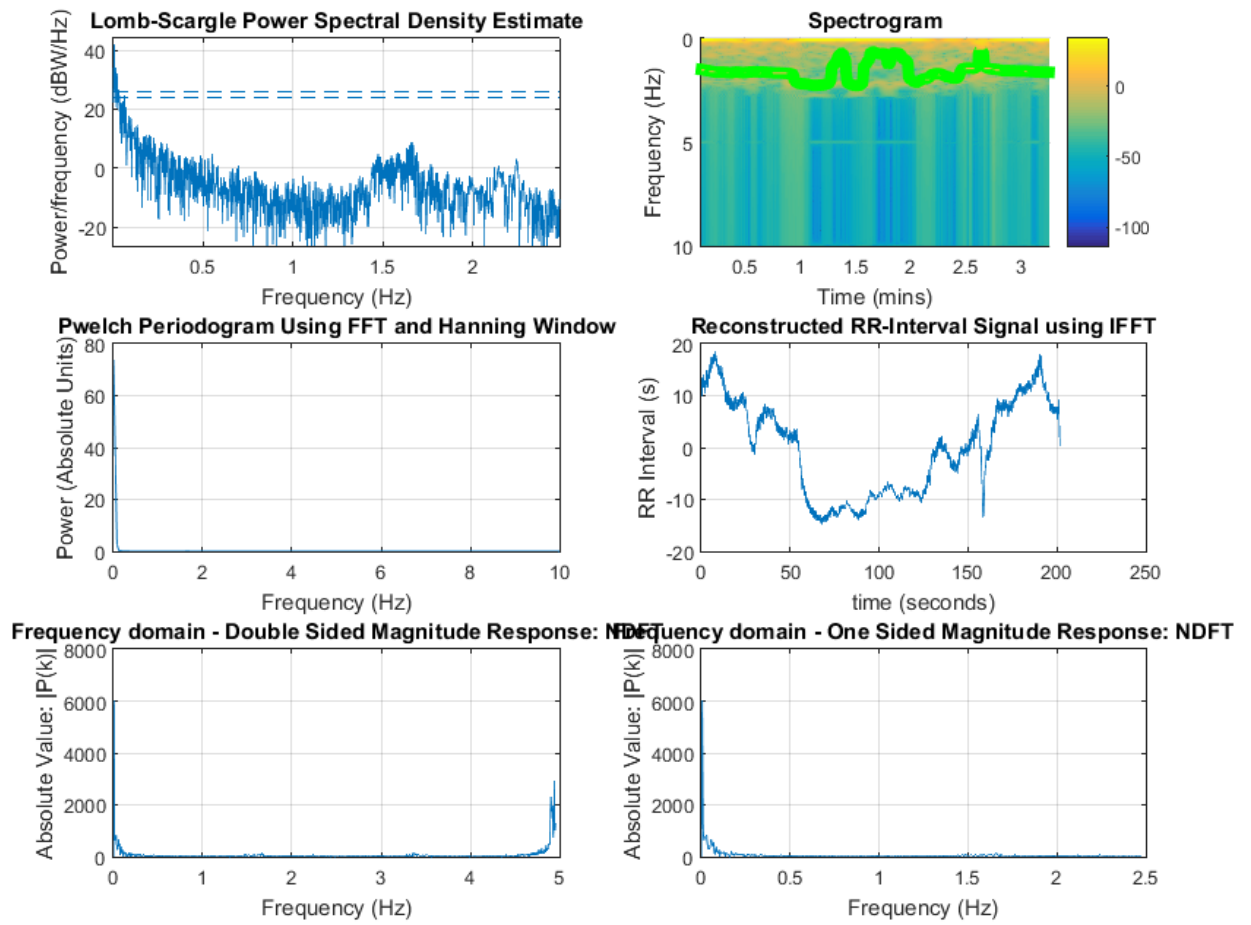
Figure 4.3: Systolic blood pressure variability spectrum for a Wistar rat

4.1.3 HRV: Time Domain

HRV was calculated using the SDNN measurement on both diabetic and control groups (figure 4.4):
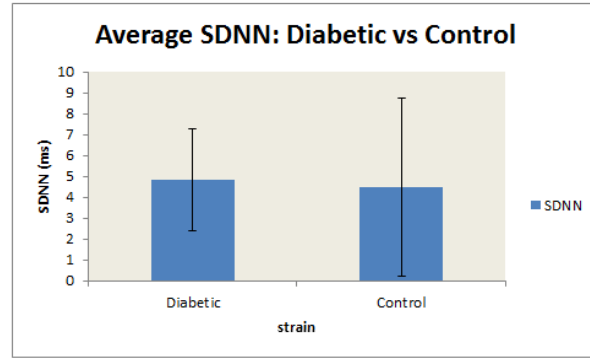
Figure 4.4: Average SDNN for diabetic and control groups ± standard deviation

4.1.4 HRV: Frequency Domain

The NDFT, LSP and welch periodograms were used to obtain the frequency spectrum of the HRV signal. Figure 4.5 shows a typical HRV signal for a diabetic rat:
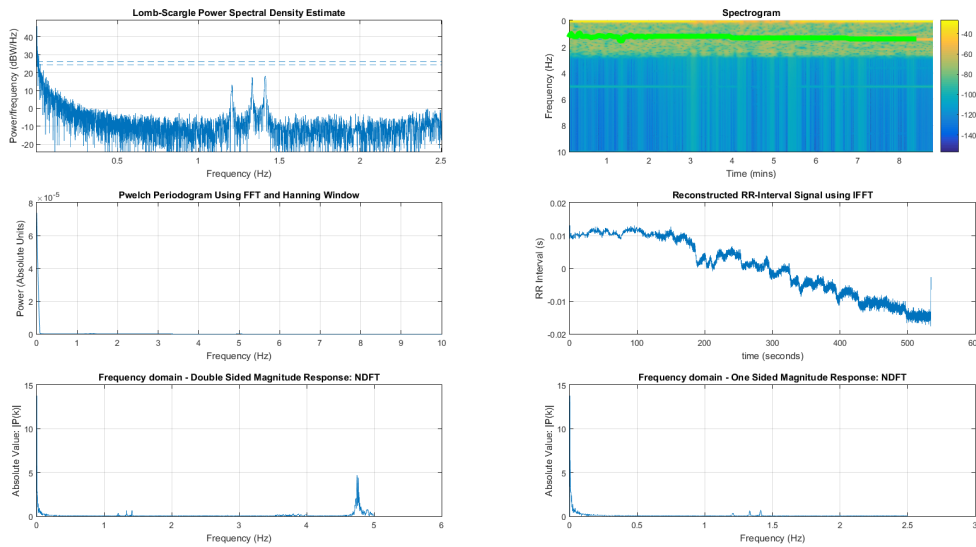
Figure 4.5: Typical HRV spectra of diabetic rats

LF (figure 4.6) and HF (figure 4.7) alpha coefficients were compared for each frequency technique to the time domain sequence technique.
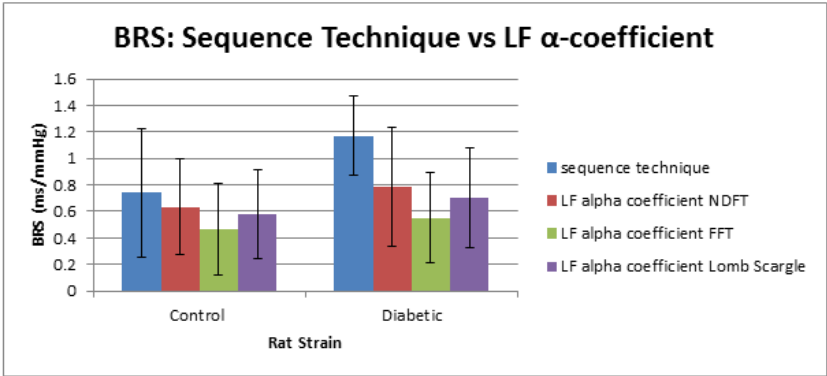
Figure 4.6: Comparison of BRS values with the LF alpha coefficient calculated from time and frequency different techniques ± standard deviation
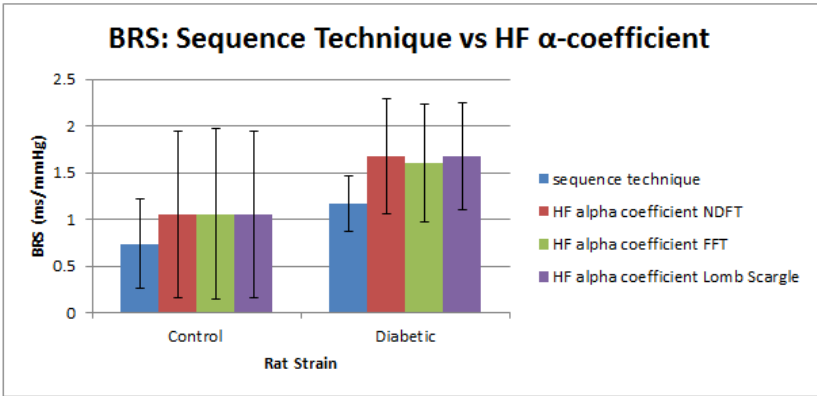
Figure 4.7: Comparison of BRS values with the HF alpha coefficient calculated from time and frequency different techniques ± standard deviation

The different frequency techniques were compared for LF and HF α-coefficients in figure 4.8:
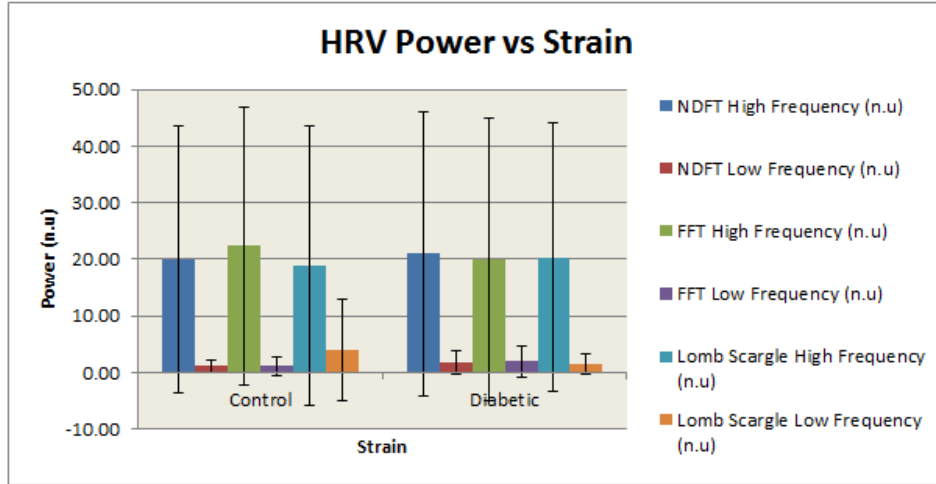
Figure 4.8: Comparison of different frequency techniques in diabetic and control rats.

4.2 Discussion

This section aims to analyse results of HRV and BRS measurements in diabetic and Wistar rats.

4.2.1 BRS in the Time Domain

BRS was calculated using the time based sequence technique. Table 4.1 that there was a significant difference between control and diabetic strains. There is enough sample data whose average and standard deviation will be representative of the whole population. One of the pitfalls of using the sequence technique that was mentioned in section 3.3 is that it takes only a narrow range of pressures. In this case however, since diabetes and hypertension are co-morbid diseases, it stands to reason that regardless of whether pharmacological or time domain methods are used, there is likely be a significant difference in BRS between strains.

4.2.2 HRV in the Time Domain

Figure 4.4 shows the average SDNN for diabetic and control strains. Initially one can say that there is not much of a difference between the SDNN values, but the standard deviation is larger for the control population. We can say that the spread of SDNN values over the sample population of Wistar rats is larger than diabetic rats. This could be indicative of higher HRV in Wistar rats than in diabetic rats.

4.3 BRS in the Frequency Domain

Figure 4.2 shows an example of the various frequency domain techniques used to find the autonomic components of HRV. As outlined in section 3.4, there is the 'mixing' effect of frequencies present between the low frequency band and the respiratory frequency in the spectrogram. The FFT, NDFT and LSP give similar results. Figures 4.6 and 4.7 shows how the various frequency and time domain techniques compare when calculating the LF and HF α-coefficient, giving similar results.

4.4 HRV in the Frequency Domain

Figure 4.8 shows the LF and HF powers in normalised units for the various techniques used. There is a very large spread of data, and warrants further investigation. The power for the frequency techniques are quite similar.

4.5 Discussion of Techniques Used

Many studies such as [35], [36], [37], [38] and commercially available software packages such as [39], [40], [41] use the interpolated windowed FFT algorithm for HRV calculations. The interpolated windowed FFT is an *estimate* of the RR-interval and SBP pulse data. Therefore, the FFT was used this thesis in comparison to existing literature and to more accurate methods such as the LS periodogram. To the author's knowledge, there has been no studies to date investigating the use of the NDFT algorithm in HRV and BRS studies. Alternate methods of calculating frequency spectra includes the spectrum of intervals and the spectrum of counts [42].

Chapter 5

Conclusion

This thesis aimed to validate the use of several different frequency spectrum methods in quantifying BRS and HRV in different experimental settings. The main limitation of this study was the low number of rats used. The following conclusions were drawn from this study:

- The NDFT, LSP and FFT are suitable techniques for obtaining HRV and BRS spectra as they give similar spectral components and power.

- The sequence technique needs to be used with some caution as it measures BRS over short blood pressure ranges. In this study, the sequence technique gave different results of BRS for stimulated/non-stimulated WKY and SHR rats compared to the pharmacological method

- Despite stimulation, spontaneous sequences are still detected

- Both the respiratory, sympathetic and parasympathetic frequencies will affect the same part of the HRV spectra.

- The temporal variation of HRV can be seen in the higher harmonics of the frequency spectra of a complete ECG

- There was a significant difference between the BRS in control and diabetic rats using the sequence technique

- Stimulated normotensive rats show a marked skewness in the shape of the histogram compared to the hypertensive rats, which was a novel observation.

5.1   Future Work

Future work includes investigating the NDFT with a window function and gathering more rat data so any analysis will be suitably powered statistically.

Bibliography

[1] Z. Kouchaki, D. Georgakopoulos, M. Butlin, and A. Avolio, "Field stimulation of the carotid baroreceptor complex does not compromise baroreceptor function in spontaneously hypertensive rats," in *Engineering in Medicine and Biology Society (EMBC), 2014 36th Annual International Conference of the IEEE*, Aug 2014, pp. 2944–2945.

[2] J. Hall and A. Guyton, *Guyton and Hall Textbook of Medical Physiology*, ser. Guyton Physiology Series. Saunders/Elsevier, 2011. [Online]. Available: http://books.google.com.au/books?id=di5PtQAACAAJ

[3] W. H. Organization *et al.*, "A global brief on hypertension. silent killer, global public health crisis. geneva, switzerland: World health organization; 2013," *WHO document number WHO/DCQ/WHD/2013.2, available on the Internet at: http://www. apps. who. int/iris/bitstream/10665/79059/1/WHO_ DCO_WHD*, pp. 1–40, 2013.

[4] A. V. Chobanian, G. L. Bakris, H. R. Black, W. C. Cushman, L. A. Green, J. L. Izzo, D. W. Jones, B. J. Materson, S. Oparil, J. T. Wright, E. J. Roccella, and the National High Blood Pressure Education Program Coordinating Committee, "Seventh report of the joint national committee on prevention, detection, evaluation, and treatment of high blood pressure," *Hypertension*, vol. 42, no. 6, pp. 1206–1252, 2003. [Online]. Available: http://hyper.ahajournals.org/content/42/6/1206.abstract

[5] E. Grossman, "Blood pressure: The lower, the better: The con side," *Diabetes Care*, vol. 34, no. Supplement 2, pp. S308–S312, 2011. [Online]. Available: http://care.diabetesjournals.org/content/34/Supplement_2/S308.short

[6] Study confirms benefits of lower blood pressure. [Online]. Available: http://www.lifeclinic.com/fullpage.aspx?prid=510799&type=1

[7] R. M. Cooper-DeHoff and J. H. Karnes, "Antihypertensive medications: Benefits of blood pressure lowering and hazards of metabolic effects." *Expert Review of Cardiovascular Therapy*, vol. 7, no. 6, pp. 689–702, June 2009. [Online]. Available: http://www.ncbi.nlm.nih.gov/pmc/articles/PMC2799117/

[8] D. A. Calhoun, D. Jones, S. Textor, D. C. Goff, T. P. Murphy, R. D. Toto, A. White, W. C. Cushman, W. White, D. Sica, K. Ferdinand, T. D. Giles, B. Falkner, and R. M. Carey, "Resistant Hypertension: Diagnosis, Evaluation,

and Treatment: A Scientific Statement From the American Heart Association Professional Education Committee of the Council for High Blood Pressure Research," *Hypertension*, vol. 51, no. 6, pp. 1403–1419, 2008. [Online]. Available: http://hyper.ahajournals.org/content/51/6/1403.abstract

[9] J. D. Davidson, Andrew C.; Bisognano, "Interventional approaches for resistant hypertension." *Current Opinion in Nephrology & Hypertension.*, vol. 21, no. 5, pp. 475–480, September 2012.

[10] W. F. Boron and E. L. Boulpaep, *Medical physiology : a cellular and molecular approach*, updated ed. Philadelphia, Pa. : Elsevier Saunders, 2005.

[11] P. Richard E. Klabunde. [Online]. Available: http://cvphysiology.com/Blood%20Pressure/BP012.htm

[12] L. M. Berne RM, *Cardiovascular Physiology*. Mosby Inc., 2001.

[13] S. Oparil, M. A. Zaman, and D. A. Calhoun, "Pathogenesis of hypertension," *Annals of Internal Medicine*, vol. 139, no. 9, pp. 761–776, 2003.

[14] B. P. Olumide Olatubosun Rowaiye, Ewa Anita Jankowska, "Baroreceptor sensitivity and diabetes mellitus," *Cardiology Journal*, vol. 20, no. 5, pp. 453–463, 2013.

[15] V. E. Papaioannou, "Heart rate variability, baroreflex function and heart rate turbulence: Possible origin and implications," *Hellenic Journal of Cardiology*, vol. 48, pp. 278–289, 2007.

[16] M. J. C. Philip I. Aaronson, Jeremy P. T. Ward, *The Cardiovascular System at a Glance*. John Wiley and Sons Ltd, 2012.

[17] Medicore. Sa-300p clinical manual ver 3.0. Medicore. [Online]. Available: http://medi-core.com/download/HRV_clinical_manual_ver3.0.pdf

[18] G. G. Berntson, J. T. Bigger, D. L. Eckberg, P. Grossman, P. G. Kaufmann, M. Malik, H. N. Nagaraja, S. W. Porges, J. P. Saul, P. H. Stone *et al.*, "Heart rate variability: origins, methods, and interpretive caveats," *Psychophysiology*, vol. 34, no. 6, pp. 623–648, 1997.

[19] T. Denison, M. Morris, and F. Sun, "Building a bionic nervous system," *Spectrum, IEEE*, vol. 52, no. 2, pp. 32–39, February 2015.

[20] I. J. Scheffers, A. A. Kroon, J. Schmidli, J. Jordan, J. J. Tordoir, M. G. Mohaupt, F. C. Luft, H. Haller, J. Menne, S. Engeli, J. Ceral, S. Eckert, A. Erglis, K. Narkiewicz, T. Philipp, and P. W. de Leeuw, "Novel baroreflex activation therapy in resistant hypertension: Results of a european multi-center feasibility study," *Journal of the American College of Cardiology*, vol. 56, no. 15, pp. 1254 – 1258, 2010. [Online]. Available: http://www.sciencedirect.com/science/article/pii/S0735109710027221

[21] J. D. Bisognano, G. Bakris, M. K. Nadim, L. Sanchez, A. A. Kroon, J. Schafer, P. W. de Leeuw, and D. A. Sica, "Baroreflex activation therapy lowers blood pressure in patients with resistant hypertension: Results from the double-blind, randomized, placebo-controlled rheos pivotal trial," *Journal of the American College of Cardiology*, vol. 58, no. 7, pp. 765 – 773, 2011. [Online]. Available: http://www.sciencedirect.com/science/article/pii/S0735109711021826

[22] T. Hickethier, M. Halbach, N. Madershahian, U. V. R. Brandt, M.C. Hoppe, E. Lovett, and M. Mueller-Ehmsen, "Abstract 15717: Acute on/off effects of baroreceptor activation therapy (bat) on blood pressure after long-term therapy for resistant hypertension: Single-center experience with the barostim neo system," presented at the Crculation, American Heart Association 2013 Scientific Sessions and Resuscitation Science Symposium. American Heart Association, November 2013. [Online]. Available: http://circ.ahajournals.org/cgi/content/meeting_abstract/128/22_MeetingAbstracts/A15717

[23] P. W. de Leeuw, T. Alnima, E. Lovett, D. Sica, J. Bisognano, H. Haller, and A. A. Kroon, "Bilateral or unilateral stimulation for baroreflex activation therapy," *Hypertension*, vol. 65, no. 1, pp. 187–192, 2015. [Online]. Available: http://hyper.ahajournals.org/content/65/1/187.abstract

[24] T. F. of the European Society of Cardiology *et al.*, "Heart rate variability standards of measurement, physiological interpretation, and clinical use," *Eur Heart J*, vol. 17, pp. 354–381, 1996.

[25] M. G. Parati, Gianfranco;Di Rienzo, "How to measure baroreflex sensitivity: from the cardiovascular laboratory to daily life," *Journal of Hypertension:*, vol. 18, no. 1, 2000.

[26] G. Bertinieri, M. Di Rienzo, A. Cavallazzi, A. U. Ferrari, A. Pedotti, and G. Mancia, "Evaluation of baroreceptor reflex by blood pressure monitoring in unanesthetized cats," *American Journal of Physiology - Heart and Circulatory Physiology*, vol. 254, no. 2, pp. H377–H383, 1988. [Online]. Available: http://ajpheart.physiology.org/content/254/2/H377

[27] P. B. Persson, M. DiRienzo, P. Castiglioni, C. Cerutti, M. Pagani, N. Honzikova, S. Akselrod, and G. Parati, "Time versus frequency domain techniques for assessing baroreflex sensitivity," *Journal of Hypertension*, vol. 19, no. 10, pp. –, 2001. [Online]. Available: http://journals.lww.com/jhypertension/Fulltext/2001/10000/Time_versus_frequency_domain_techniques_for_1.aspx

[28] G. Parati, S. Omboni, A. Frattola, M. Di Rienzo, A. Zanchetti, and G. Mancia, "Dynamic evaluation of the baroreflex in ambulant subjects." *Blood pressure and heart rate variability*, pp. 123–137, 1992.

[29] S. Bagchi and S. Mitra, "The nonuniform discrete fourier transform," in *Nonuniform Sampling*, ser. Information Technology: Transmission, Processing, and Storage, F. Marvasti, Ed. Springer US, 2001, pp. 325–360. [Online]. Available: http://dx.doi.org/10.1007/978-1-4615-1229-5_7

[30] D. Bland, T. Laakso, and A. Tarczynski, "Analysis of algorithms for nonuniform-time discrete fourier transform," in *Circuits and Systems, 1996. ISCAS '96., Connecting the World., 1996 IEEE International Symposium on*, vol. 2, May 1996, pp. 453–456 vol.2.

[31] B. Fisher. Definition of non-uniform discrete fourier transform (ndft). [Online]. Available: http://homepages.inf.ed.ac.uk/rbf/CVonline/LOCAL_COPIES/PIRODDI1/NUFT/node4.html

[32] (2015) Sample size calculator. [Online]. Available: https://www.dssresearch.com/KnowledgeCenter/toolkitcalculators/samplesizecalculators.aspx

[33] G. Milicevi, "Low to high frequency ratio of heart rate variability spectra fails to describe sympatho-vagal balance in cardiac patients," *Collegium antropologicum*, vol. 29, no. 1, pp. 295–300, 2005.

[34] G. E. Billman, "The lf/hf ratio does not accurately measure cardiac sympatho-vagal balance," *Frontiers in Physiology*, vol. 4, no. 26, February 2013, opinion Article.

[35] M. Peltola, "Role of editing of rr intervals in the analysis of heart rate variability." *Frontiers in Physiology*, vol. 3, no. 148, 2012.

[36] A. P. Pichon, C. De Bisschop, M. Roulaud, A. Denjean, and Y. Papelier, "Spectral analysis of heart rate variability during exercise in trained subjects," *Medicine & Science in Sports & Exercise*, vol. 36, no. 10, pp. –, 2004. [Online]. Available: http://journals.lww.com/acsm-msse/Fulltext/2004/10000/Spectral_Analysis_of_Heart_Rate_Variability_during.7.aspx

[37] G. V. Mendonca, B. Fernhall, K. S. Heffernan, and F. D. Pereira, "Spectral methods of heart rate variability analysis during dynamic exercise," *Clinical Autonomic Research*, vol. 19, no. 4, pp. 237–245, 2009. [Online]. Available: http://dx.doi.org/10.1007/s10286-009-0018-1

[38] J. Niskanen, M. Tarvainen, P. Ranta-Aho, and P. Karjalainen, "Software for advanced hrv analysis." *Comput Methods Programs Biomed.*, vol. 76, no. 1, pp. 73–81, Oct 2004.

[39] G. Wilkins. Using the lomb-scargle periodogram for hrv analysis. [Online]. Available: http://www.adinstruments.com/blog/using-lomb-scargle-periodogram-hrv-analysis

[40] (2012, September) Using labview for heart rate variability analysis. [Online]. Available: http://www.ni.com/example/30832/en/

[41] (2015, May) Hrv in labchart 7 vs. 8. [Online]. Available: http://forum.adinstruments.com/viewtopic.php?f=7&t=685

[42] R. W. DeBoer, J. M. Karemaker, and J. Strackee, "Comparing spectra of a series of point events particularly for heart rate variability data," *Biomedical Engineering, IEEE Transactions on*, vol. BME-31, no. 4, pp. 384–387, April 1984.

[43] G. Grassi, A. Mark, and M. Esler, "The sympathetic nervous system alterations in human hypertension," *Circulation Research*, vol. 116, no. 6, pp. 976–990, 2015. [Online]. Available: http://circres.ahajournals.org/content/116/6/976.abstract

[44] S. Oparil and R. E. Schmieder, "New approaches in the treatment of hypertension," *Circulation Research*, vol. 116, no. 6, pp. 1074–1095, 2015. [Online]. Available: http://circres.ahajournals.org/content/116/6/1074.abstract

[45] K. Rahimi, C. A. Emdin, and S. MacMahon, "The epidemiology of blood pressure and its worldwide management," *Circulation Research*, vol. 116, no. 6, pp. 925–936, 2015. [Online]. Available: http://circres.ahajournals.org/content/116/6/925.abstract

[46] A. Steptoe and C. Vögele, "Cardiac baroreflex function during postural change assessed using non-invasive spontaneous sequence analysis in young men," *Cardiovascular Research*, vol. 24, no. 8, pp. 627–632, 1990.

[47] N. Westerhof, N. Stergiopulos, and M. Noble, *Snapshots of Hemodynamics: An Aid for Clinical Research and Graduate Education*, ser. SpringerLink : Bücher. Springer, 2010. [Online]. Available: http://books.google.com.au/books?id=fqWIm8RmVYsC

[48] K. Wustmann, J. P. Kucera, I. Scheffers, M. Mohaupt, A. A. Kroon, P. W. de Leeuw, J. Schmidli, Y. Allemann, and E. Delacrtaz, "Effects of chronic baroreceptor stimulation on the autonomic cardiovascular regulation in patients with drug-resistant arterial hypertension," *Hypertension*, vol. 54, no. 3, pp. 530–536, 2009. [Online]. Available: http://hyper.ahajournals.org/content/54/3/530.abstract

Appendix A

Matlab Code

A.1 Calling File for Sequences

```matlab
1 % time_seconds = xlsread('SHR_100314.xlsx','SHR_stim','B2:B1623'); ...
      %in seconds
2 RR_Interval = xlsread('nostim.csv','K2:K1769'); % ms
3 SP = xlsread('nostim.csv','W2:W1769'); %SP2: taken abdominally
4
5 % Thresholds
6 SBP_threshold = 1; %mmHg
7 RR_Interval_threshold = 1; %ms
8
9 a = zeros(8,1);
10 hSub = zeros(8,1);
11
12 [slopes1,a(1),average1]= ...
      negative_sequences_with_plots_lag0(SBP_threshold,...
13      RR_Interval_threshold,SP,RR_Interval);
14 [slopes2,a(2),average2]= ...
      negative_sequences_with_plots_lag1(SBP_threshold,...
15      RR_Interval_threshold,SP,RR_Interval);
16 [slopes3,a(3),average3]= ...
      negative_sequences_with_plots_lag2(SBP_threshold,...
17      RR_Interval_threshold,SP,RR_Interval);
18 [slopes4,a(4),average4]= ...
      negative_sequences_with_plots_lag3(SBP_threshold,...
19      RR_Interval_threshold,SP,RR_Interval);
20 [slopes5,a(5),average5]= ...
      positive_sequences_with_plots_lag0(SBP_threshold,...
21      RR_Interval_threshold,SP,RR_Interval);
22 [slopes6,a(6),average6]= ...
      positive_sequences_with_plots_lag1(SBP_threshold,...
23      RR_Interval_threshold,SP,RR_Interval);
24 [slopes7,a(7),average7]= ...
      positive_sequences_with_plots_lag2(SBP_threshold,...
```

```matlab
25      RR_Interval_threshold,SP,RR_Interval);
26  [slopes8,a(8),average8]= ...
        positive_sequences_with_plots_lag3(SBP_threshold,...
27      RR_Interval_threshold,SP,RR_Interval);
28
29  fig = figure;
30  for i = 1:8
31      subplot(4,2,i)
32      xlabel ('Systolic Blood Pressure (mmHg)')
33      ylabel('RR Interval (ms)')
34  %    textul('No Sequences');
35  %    suptitle( 'I''m a super title');
36      if( i == 1)
37          str = sprintf('Negative Sequences (Lag 0), BRS = ...
                %0.2f',average1);
38          title(str);
39          hSub(1) = subplot(4,2,i);
40      elseif (i == 2)
41          str = sprintf('Negative Sequences (Lag 1), BRS = %0.2f',average2);
42          title(str);
43          hSub(2) = subplot(4,2,i);
44      elseif (i == 3)
45          str = sprintf('Negative Sequences (Lag 2), BRS = %0.2f', ...
                average3);
46          title(str);
47          hSub(3) = subplot(4,2,i);
48      elseif (i == 4)
49          str = sprintf('Negative Sequences (Lag 3), BRS = %0.2f', ...
                average4);
50          title(str);
51           hSub(4) = subplot(4,2,i);
52      elseif (i == 5)
53          str = sprintf('Positive Sequences (Lag 0), BRS = %0.2f',average5);
54          title(str);
55           hSub(5) = subplot(4,2,i);
56      elseif (i == 6)
57          str = sprintf('Positive Sequences (Lag 1), BRS = %0.2f',average6);
58          title(str);
59           hSub(6) = subplot(4,2,i);
60      elseif (i == 7)
61          str = sprintf('Positive Sequences (Lag 2), BRS = %0.2f', ...
                average7);
62          title(str);
63           hSub(7) = subplot(4,2,i);
64      elseif (i == 8)
65          str = sprintf('Positive Sequences (Lag 3), BRS = %0.2f', ...
                average8);
66          title(str);
67           hSub(8) = subplot(4,2,i);
68      end
69      i = i + 1;
70  end
```

```
71
72  for i = 1:8
73      if(a(i) == 0)
74          continue;
75      else
76          fig1 = get(a(i),'children');
77          copyobj(fig1,hSub(i));
78      end
79  end
```

A.2 Negative Sequences Lag 1

```
1  function[slopes2,a,average_BRS2] = ...
       negative_sequences_with_plots_lag1(SBP_threshold, ...
       RR_Interval_threshold,SP,RR_Interval)
2  slopes2 = [];
3  average_BRS2 = 0;
4  a = 0;
5  % program for determining Baroreceptor Sensitivity (BRS) in rats
6  % using the sequence technique
7  % written by Harish Ramachandran
8  % Master of Research (MRes) Student
9  % 17/03/2015
10
11 RR_Interval = RR_Interval*1000;%ms
12 B = [NaN NaN; NaN NaN];
13 concat_data = [SP,RR_Interval];
14 concat_data = vertcat(concat_data,B);
15 [num_rows,num_cols] = size(concat_data);
16 max_number_zeros = ceil(num_rows/3);
17 sequence_holder = zeros(max_number_zeros+num_rows,num_cols);
18 sequence_element = 1; % one line of data constitutes ONE sequence element
19 num_sequences = 0;
20
21 for c = 1:num_rows-1
22     if (concat_data(c+1,1)-concat_data(c,1)) < 0 && ...
23         abs(concat_data(c+1,1)-concat_data(c,1))>= SBP_threshold
24           if (concat_data(c+2,num_cols)-concat_data(c+1,num_cols)) < 0 ...
                  && ...
25               abs(concat_data(c+2,num_cols)-concat_data(c+1,num_cols))...
26               >= RR_Interval_threshold
27           sequence_element = sequence_element + 1;
28           elseif ...
                  abs(concat_data(c+2,num_cols)-concat_data(c+1,num_cols))...
29               < (RR_Interval_threshold) || ...
30               (concat_data(c+2,num_cols)-concat_data(c+1,num_cols)) > 0
31               if sequence_element >= 3
32               num_sequences = num_sequences + 1;
```

```
33              fprintf('Sequence Number %d has %d consecutive ...
                   elements\n',num_sequences,sequence_element);
34              for d = c-sequence_element+1:c
35                      sequence_holder(d,1) = concat_data(d,1);
36                      sequence_holder(d,num_cols) = ...
                           concat_data(d+1,num_cols);
37              end
38              sequence_element = 1;
39                  continue;
40              else
41                  sequence_element = 1;
42                  continue;
43              end
44          end
45      elseif (concat_data(c+1,1)-concat_data(c,1)) >= 0
46  %           && ...
47  %               abs(concat_data(c+1,1)-concat_data(c,1)) < SPB_threshold
48          if sequence_element >= 3
49              num_sequences = num_sequences + 1;
50              fprintf('Sequence Number %d has %d consecutive ...
                   elements\n',num_sequences,sequence_element);
51              for d = c-sequence_element+1:c
52                      sequence_holder(d,1) = concat_data(d,1);
53                      sequence_holder(d,num_cols) = ...
                           concat_data(d+1,num_cols);
54              end
55              sequence_element = 1;
56          else
57              sequence_element = 1;
58          continue;
59          end
60      else
61          sequence_element = 1;
62          continue;
63      end
64  end
65
66  if num_sequences == 0
67      fprintf('No sequences found.\n');
68      return;
69  end
70
71  % create cell array
72  rows = find(any(sequence_holder,2));
73  blocklengths = diff(find([1;diff(rows)>1;1]));
74  blocks = mat2cell(sequence_holder(rows,:),blocklengths);
75
76  fig = figure;
77  hold all
78
79  slopes2 = [];
80  %plot figures
```

```matlab
81  %   for d = 1:length(blocks)
82  %       g = blocks{d};
83  %       plot(g(:,1),g(:,2),'--o')
84  %       title('Positive Sequences');
85  %       xlabel('systolic blood pressure (mmHg)');
86  %       ylabel('RR Interval (ms)');
87  %   end
88  %  hold off;
89   for d = 1:length(blocks)
90       g = blocks{d};
91       P = polyfit(g(:,1),g(:,2),1);
92       slopes2(d) = P(1);
93       f = polyval(P,g(:,1));
94       plot(g(:,1),f,'--o')
95       title('Negative Sequences (Lag 1)');
96       xlabel('Systolic Blood Pressure (mmHg)');
97       ylabel('RR Interval (ms)');
98      [fitobject, gof] = fit(g(:,1),g(:,2), 'poly1');
99       fprintf('regression value is %d\n',gof.rsquare)
100  end
101  hold off;
102
103  %get handle to axis of current figure;
104  a = gca;
105  slopes2 = slopes2';
106  average_BRS2 = mean(slopes2)
```

A.3   Positive Sequences Lag 3

```matlab
1  function[slopes8,a,average_BRS8] = ...
       positive_sequences_with_plots_lag3(SBP_threshold, ...
       RR_Interval_threshold,SP,RR_Interval)
2  slopes8 = [];
3  average_BRS8 = 0;
4  a = 0;
5  % program for determining Baroreceptor Sensitivity (BRS) in rats
6  % using the sequence technique
7  % written by Harish Ramachandran
8  % Master of Research (MRes) Student
9  % 17/03/2015
10
11  RR_Interval = RR_Interval*1000;%ms
12  B = [NaN NaN; NaN NaN; NaN NaN;NaN NaN];
13  concat_data = [SP,RR_Interval];
14  concat_data = vertcat(concat_data,B);
15  [num_rows,num_cols] = size(concat_data);
16  max_number_zeros = ceil(num_rows/3);
17  sequence_holder = zeros(max_number_zeros+num_rows,num_cols);
```

```matlab
18  sequence_element = 1; % one line of data constitutes ONE sequence element
19  num_sequences = 0;
20
21  for c = 1:num_rows-1
22      if (concat_data(c+1,1)-concat_data(c,1)) >= SBP_threshold
23          if (concat_data(c+4,num_cols)-concat_data(c+3,num_cols))...
24              >= RR_Interval_threshold
25          sequence_element = sequence_element + 1;
26          elseif (concat_data(c+4,num_cols)-concat_data(c+3,num_cols))...
27              < RR_Interval_threshold
28              if sequence_element >= 3
29              num_sequences = num_sequences + 1;
30              fprintf('Sequence Number %d has %d consecutive ...
                    elements\n',num_sequences,sequence_element);
31                  for d = c-sequence_element+1:c
32                      sequence_holder(d,1) = concat_data(d,1);
33                      sequence_holder(d,num_cols) = ...
                            concat_data(d+3,num_cols);
34                  end
35              sequence_element = 1;
36                  continue;
37              else
38                  sequence_element = 1;
39                  continue;
40              end
41          end
42      elseif (concat_data(c+1,1)-concat_data(c,1)) < SBP_threshold
43          if sequence_element >= 3
44              num_sequences = num_sequences + 1;
45              fprintf('Sequence Number %d has %d consecutive ...
                    elements\n',num_sequences,sequence_element);
46              for d = c-sequence_element+1:c
47                      sequence_holder(d,1) = concat_data(d,1);
48                      sequence_holder(d,num_cols) = ...
                            concat_data(d+3,num_cols);
49              end
50              sequence_element = 1;
51          else
52              sequence_element = 1;
53              continue;
54          end
55      end
56  end
57
58  if num_sequences == 0
59      fprintf('No sequences found.\n');
60      return;
61  end
62
63  % create cell array
64  rows = find(any(sequence_holder,2));
65  blocklengths = diff(find([1;diff(rows)>1;1]));
```

```matlab
66  blocks = mat2cell(sequence_holder(rows,:),blocklengths);
67
68  fig = figure;
69  hold all
70
71  slopes8 = [];
72  %plot figures
73  %  for d = 1:length(blocks)
74  %      g = blocks{d};
75  %      plot(g(:,1),g(:,2),'--o')
76  %      title('Positive Sequences');
77  %      xlabel('systolic blood pressure (mmHg)');
78  %      ylabel('RR Interval (ms)');
79  %  end
80  %  hold off;
81
82   for d = 1:length(blocks)
83       g = blocks{d};
84       P = polyfit(g(:,1),g(:,2),1);
85       slopes8(d) = P(1);
86       f = polyval(P,g(:,1));
87       plot(g(:,1),f,'--o')
88       title('Positive Sequences (Lag 3)');
89       xlabel('systolic blood pressure (mmHg)');
90       ylabel('RR Interval (ms)');
91      [fitobject, gof] = fit(g(:,1),g(:,2), 'poly1');
92       fprintf('regression value is %d\n',gof.rsquare)
93   end
94   hold off;
95
96    %get axis handle to figure
97   a = gca;
98   slopes8 = slopes8';
99   average_BRS8 = mean(slopes8)
```

A.4   Frequency Analysis

```matlab
1  %% Read in Data
2
3  time_seconds = xlsread('stim.csv','B2:B1740'); %in seconds
4  RR_Interval = xlsread('stim.csv','K2:K1740'); % ms
5
6  %% %% Method 1
7
8  Dummy_RR_Interval = RR_Interval*1000;
9  % The dashed lines denote 95% and 50% detection probabilities. These
10 % thresholds measure the statistical significance of peaks.
11 subplot(3,2,1)
```

```matlab
12  plomb(RR_Interval,time_seconds,'Pd',[0.99, 0.5]);
13  [pxx,fxx] = plomb(Dummy_RR_Interval,time_seconds,'Pd',[0.99 0.5]);
14
15  % Find the high frequency [1 3] RMS value
16
17  % find indices
18  %start
19  st = find(fxx <= 1);
20  st = st(end);
21
22  %finish
23  e = find(fxx <= 3);
24  e = e(end);
25
26  hxx = pxx(st:e);%in dBW
27
28  Power = sum(hxx,1);
29  %
30  HFP = Power;
31
32  fprintf('Lomb-Scargle Periodogram HFP: %d ms^2\n',HFP);
33
34  % find indices
35
36  % start
37  st = find(fxx <= 0.2);
38  st = st(end);
39
40  %finish
41  e = find(fxx <= 1);
42  e = e(end);
43
44  % Find the low frequency [0.2 0.95] RMS value
45
46  lxx = pxx(st:e);
47
48  Power = sum(lxx,1);
49  LFP = Power;
50
51  fprintf('Lomb-Scargle Periodogram LFP: %d ms^2\n',LFP);
52
53  % find VLF
54
55  st = find(fxx<=0.04);
56  st = st(end);
57
58  %finish
59
60  e = find(fxx <= 0.2);
61  e = e(end);
62
63  vlxx = pxx(st:e);
```

```matlab
64
65  % Actual_power = 10.^(vlxx/10);
66
67  % vlxx = vlxx.^2;
68
69  Power = sum(vlxx,1);
70  VLP = Power;
71
72  fprintf('Lomb-Scargle Periodogram VLP: %d ms^2\n',VLP);
73
74  % Find the total power
75  txx = pxx;
76  % Actual_power = 10.^(txx/10);
77  % txx = txx.^2;
78  Power = sum(txx,1);
79
80  TFP = Power;
81
82  fprintf('Lomb-Scargle Periodogram TFP: %d ms^2\n',TFP);
83
84  sprintf('Normalised Units\n');
85
86  fprintf('LFP normalised units: %0.3f n.u \n',(LFP/(TFP-VLP))*100);
87
88  fprintf('HFP normalised units: %0.3f n.u \n',(HFP/(TFP-VLP))*100);
89  %%  %% Method 2
90  % resample frequency
91  fs = 20;  %[Hz]
92
93  %set DC to zero
94  sbpav = mean(RR_Interval);
95  RR_Interval = RR_Interval-sbpav;
96
97  [Y,Ty] =resample(RR_Interval,time_seconds,fs); % Y is resampled ...
           RR_interval
98  [pxx,f] = pwelch(Y,512,128,512,fs,'power');
99
100 subplot(3,2,3)
101 plot(f,pxx);
102 xlabel('Frequency (Hz)');
103 ylabel('Power (Absolute Units)');
104 title('Pwelch Periodogram Using FFT and Hanning Window');
105 grid on;
106
107 % Find the high frequency [1 3] RMS value
108
109 % find indices
110 %start
111 st = find(f <= 1);
112 st = st(end);
113
114 %finish
```

```matlab
115  e = find(f <= 3);
116  e = e(end);
117
118  hxx = pxx(st:e);%in dBW
119  Power = sum(hxx,1);
120  %
121  HFP = Power*1e6;
122
123  fprintf('Pwelch Periodogram HFP: %d ms^2\n',HFP);
124
125  % find indices
126
127  % start
128  st = find(f <= 0.2);
129  st = st(end);
130
131  %finish
132  e = find(f <= 1);
133  e = e(end);
134
135  % Find the low frequency [0.2 0.95] RMS value
136
137  lxx = pxx(st:e);
138
139  Power = sum(lxx,1);
140  LFP = Power*1e6;
141
142  fprintf('Pwelch Periodogram LFP: %d ms^2\n',LFP);
143
144  % find VLF
145
146  st = find(f<=0.04);
147  st = st(end);
148
149  %finish
150
151  e = find(f <= 0.2);
152  e = e(end);
153
154  vlxx = pxx(st:e);
155
156  Power = sum(vlxx,1);
157  VLP = Power*1e6;
158
159  fprintf('Pwelch Periodogram VLP: %d ms^2\n',VLP);
160
161  % Find the total power
162  txx = pxx;
163  Power = sum(txx,1);
164
165  TFP = Power*1e6;
166
```

```matlab
167   fprintf('Pwelch Periodogram TFP: %d ms^2\n',TFP);
168
169   sprintf('Normalised Units\n');
170
171   fprintf('LFP normalised units: %0.3f n.u \n',(LFP/(TFP-VLP))*100);
172
173   fprintf('HFP normalised units: %0.3f n.u \n',(HFP/(TFP-VLP))*100);
174
175   % figure(2)
176   subplot(3,2,2);
177
178   spectrogram(Y,256,250,256,fs,'yaxis')
179   [s,f,t,p] = spectrogram(Y,256,250,256,fs);
180   [q,nd] = max(10*log10(p));
181   ax = gca;
182   ax.YDir = 'reverse';
183   f2 = f > 0.5;
184   t2 = t > 0 & t < 500.6;
185   m2 = medfreq(p(f2,t2),f(f2));
186
187   hold on
188   title('Spectrogram')
189   plot((t(t2)./60),m2,'g','linewidth',6)
190   hold off
191
192   % hold on
193   % plot3((t./60),f(nd),q,'r','linewidth',4)
194   % hold off
195   colorbar
196   view(2)
197
198
199   G = fft(Y);
200   I = ifft(G,'symmetric');
201
202   % figure(4)
203   subplot(324);
204   plot(Ty,I)
205   grid on;
206   xlabel('time (seconds)')
207   ylabel ('RR Interval (s)')
208   title('Reconstructed RR-Interval Signal using IFFT');
209
210
211
212   %% Method 3 My Algorithm
213
214   % time range
215   L = length(time_seconds);
216   T = time_seconds(L) - time_seconds(1);
217   % M = length(Systolic_BP);
218
```

```matlab
219  %set DC to zero
220  sbpav = mean(RR_Interval);
221  RR_Interval = RR_Interval-sbpav;
222
223  % RR_Interval = RR_Interval*1000;
224
225  concat_data = [time_seconds,RR_Interval];
226  L = length(time_seconds);
227
228  % NDFT Algorithm
229  P = zeros(L,1);
230
231  for k = 0:L-1
232      for n = 0:L-1
233          P(k+1) = P(k+1) + ...
                   RR_Interval(n+1)*exp((-1i*2*pi*time_seconds(n+1)*k/T));
234      end
235  end
236
237  % generate frequencies
238  F = ones(L,1);
239  for m = 1:L
240      F(m) = (m-1)/T; % in cycles/sec
241  end
242
243  % Two sided Frequency Spectrum
244  % figure(5)
245  subplot(325)
246  plot(F,abs(P));
247  grid on;
248  xlabel('Frequency (Hz)');
249  ylabel('Absolute Value: |P(k)|');
250  title('Frequency domain - Double Sided Magnitude Response: NDFT');
251
252  cutOff = ceil(L/2);
253
254  F = F(1:cutOff);
255  B = abs(P(1:cutOff));
256
257  % One Sided Frequency Spectrum
258  % figure(6)
259  subplot(326);
260  plot(F,B);
261  grid on;
262  xlabel('Frequency (Hz)');
263  ylabel('Absolute Value: |P(k)|');
264  title('Frequency domain - One Sided Magnitude Response: NDFT');
265
266
267  %% Power Calculations
268  % find indices
269  %start
```

```matlab
270  st = find(F <= 1);
271  st = st(end);
272
273  %finish
274  e = find(F <= 3);
275  e = e(end);
276
277  % Find the high frequency [1 3] RMS value
278  B_h = B(st:e);
279
280  B_h = B_h.^2;
281  Power = sum(B_h);
282  HFP = Power*1e6;
283
284  fprintf('NDFT HFP: %d ms^2\n',HFP);
285
286  % Find the low frequency [0.2 0.95] RMS value
287
288  % find indices
289  %start
290  st = find(F <= 0.2);
291  st = st(end);
292
293  %finish
294  e = find(F <= 1);
295  e = e(end);
296
297  B_l = B(st:e);
298  B_l = B_l.^2;
299  Power = sum(B_l);
300
301  LFP = Power*1e6;
302
303  fprintf('NDFT LFP: %d ms^2\n',LFP);
304
305  % Find the total power
306  B_t = B;
307
308  B_t = B_t.^2;
309
310  Power = sum(B_t);
311
312  TFP = Power*1e6;
313
314  fprintf('NDFT TFP: %0.3f ms^2\n',TFP);
315
316  %VLP
317
318  %start
319  st = find(F <= 0.04);
320  st = st(end);
321
```

```matlab
322  %finish
323  e = find(F <= 0.2);
324  e = e(end);
325
326  B_v = B(st:e);
327
328  B_v = B_v.^2;
329  Power = sum(B_v);
330
331  VLP = Power*1e6;
332
333  fprintf('NDFT VLP: %0.3f ms^2\n',VLP);
334
335  display('Normalised Units');
336
337  fprintf('NDFT LFP normalised units: %0.3f n.u \n',(LFP/(TFP-VLP))*100);
338
339  fprintf('NDFT HFP normalised units: %0.3f n.u \n',(HFP/(TFP-VLP))*100);
```

Appendix B

Statistical Tests

sequence vs LF lomb	BRS calculated in the time domain (ms/mmHg)				BRS calculated in the frequency domain (ms/mmHg)			
	SHR	SHR STIM	WKR	WKR STIM	LF Lomb SHR	LF Lomb SHR STIM	LF Lomb WKR	LF Lomb WKR STIM
rat 1	0.20	0.24	0.32	0.43	0.13	0.13	0.87	1.70
rat 2	0.69	0.30	0.41	1.07	0.24	0.24	0.27	1.70
rat 3			0.25	0.61			0.34	0.62
p-value	0.40	0.15	0.49	0.22				

sequence vs HF lomb	BRS calculated in the time domain (ms/mmHg)				BRS calculated in the frequency domain (ms/mmHg)			
	SHR	SHR STIM	WKR	WKR STIM	HF Lomb SHR	HF Lomb SHR STIM	HF Lomb WKR	HF Lomb WKR STIM
rat 1	0.20	0.24	0.32	0.43	0.53	0.62	0.31	0.41
rat 2	0.69	0.30	0.41	1.07	0.17	0.18	0.43	0.41
rat 3			0.25	0.61			0.21	0.44
p-value	0.86	0.69	0.61	0.28				

sequence vs LF FFT	BRS calculated in the time domain (ms/mmHg)				BRS calculated in the frequency domain (ms/mmHg)			
	SHR	SHR STIM	WKR	WKR STIM	LF FFT SHR	LF FFT SHR STIM	LF FFT WKR	LF FFT WKR STIM
rat 1	0.20	0.24	0.32	0.43	0.13	0.16	0.99	1.77
rat 2	0.69	0.30	0.41	1.07	0.22	0.85	0.28	1.77
rat 3			0.25	0.61			0.30	0.59
p-value	0.41	0.59	0.49	0.23				

sequence vs HF FFT	BRS calculated in the time domain (mmHg)				BRS calculated in the frequency domain (mmHg)			
	SHR	SHR STIM	WKR	WKR STIM	HF FFT SHR	HF FFT SHR STIM	HF FFT WKR	HF FFT WKR STIM
rat 1	0.20	0.24	0.32	0.43	0.41	0.40	0.29	0.39
rat 2	0.69	0.30	0.41	1.07	0.13	0.17	0.33	0.39
rat 3			0.25	0.61			0.20	0.36
p-value	0.73	0.92	0.08	0.23				

sequence vs HF NDFT	BRS calculated in the time domain (ms/mmHg)				BRS calculated in the frequency domain (ms/mmHg)			
	SHR	SHR STIM	WKR	WKR STIM	HF NDFT SHR	HF NDFT SHR STIM	HF NDFT WKR	HF NDFT WKR STIM
rat 1	0.20	0.24	0.32	0.43	0.63	0.51	0.31	0.63
rat 2	0.69	0.30	0.41	1.07	0.18	0.17	0.42	0.41
rat 3			0.25	0.61			0.21	0.44
p-value	0.95	0.79	0.55	0.48				

sequence vs LF NDFT	BRS calculated in the time domain (ms/mmHg)				BRS calculated in the frequency domain (ms/mmHg)			
	SHR	SHR STIM	WKR	WKR STIM	LF NDFT SHR	LF NDFT SHR STIM	LF NDFT WKR	LF NDFT WKR STIM
rat 1	0.20	0.24	0.32	0.43	0.13	0.16	0.80	0.16
rat 2	0.69	0.30	0.41	1.07	0.23	0.85	0.27	2.03
rat 3			0.25	0.61			0.32	0.63
p-value	0.40	0.59	0.51	0.60				

Figure B.1: Statistical comparison between various frequency techniques and rats strains

Appendix C

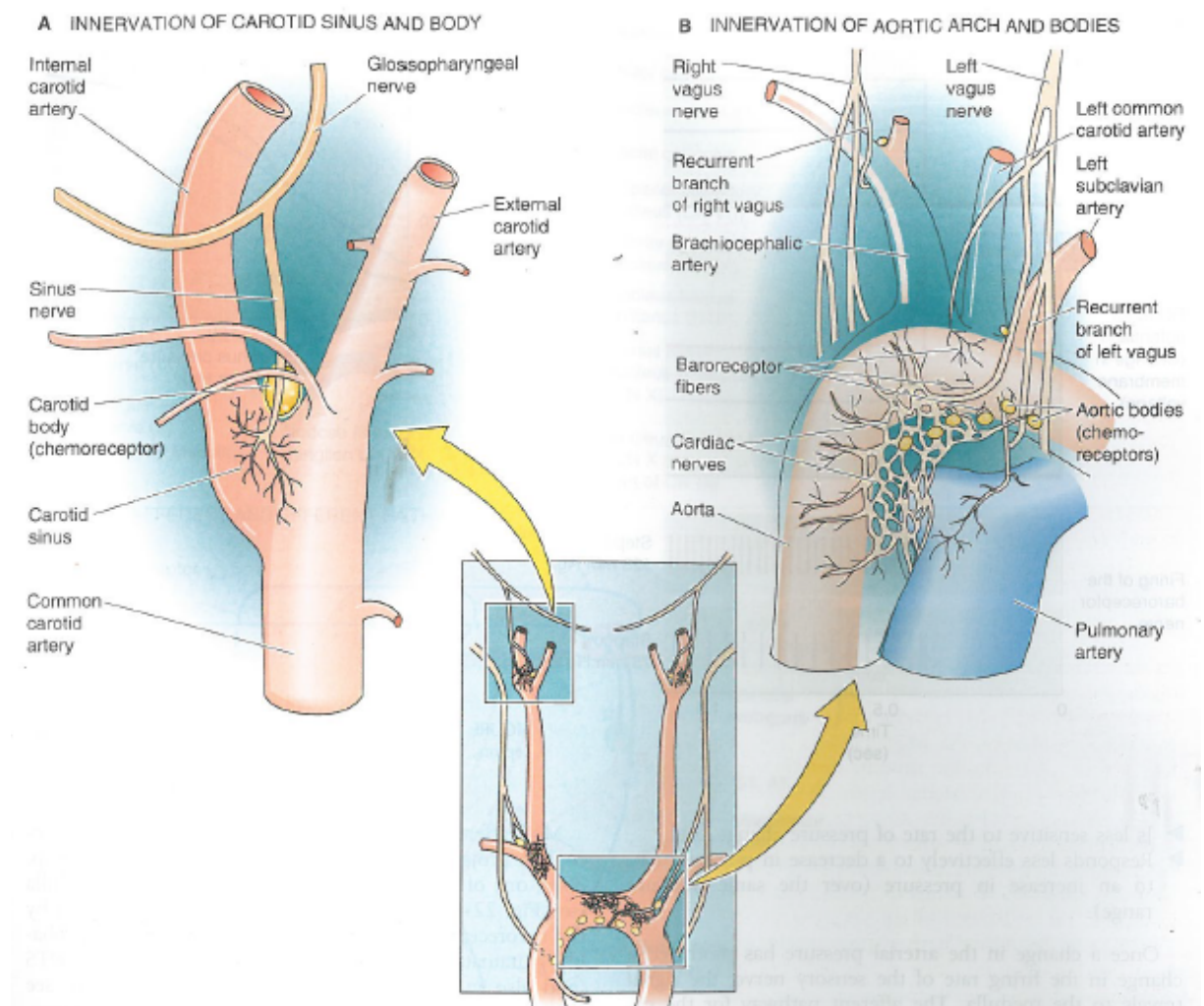# Baroreceptor Anatomy

Figure C.1: Baroreceptors in the carotid sinus and aortic arch. Diagram taken from [10].

Appendix D

Ethics Approval

D.1 Diabetic Rat Ethics Approval

ANIMAL RESEARCH AUTHORITY (ARA)

MACQUARIE UNIVERSITY

AEC Reference No.: 2012/022 - 2   **Date of Expiry:**   30 April 2013

Full Approval Duration: *01 May 2012 to 30 April 2013 (12 Months)*

Principal Investigator:
Mark Butlin
ASAM
Mark.butlin@mq.edu.au
0422 908 895

Associate Investigators:
Erik Salum   +37 253 414 199
Alberto Alvolio   0408 657 616

<div style="border:1px solid red">

In case of emergency, please contact:

the Principal Investigator / Associate Investigator named above

Or Manager, CAHF: 9850 7780 / 0428 861 163 and **Animal Welfare Officer**: 9850 7758 / 0439 497 383

</div>

The above-named are authorised by MACQUARIE UNIVERSITY ANIMAL ETHICS COMMITTEE to conduct the following research:

Title of the project: **The effect of diabetes and diabetes with antihypertensive treatment, on large artery stiffness**

Purpose: **4: research: Human or animal biology**

Aims: **This project aims to study the parameters of aortic stiffness in a rodent model of diabetes, with anti-hypertensive treatment.**

Surgical Procedures category: 2: animal unconscious without recovery; 3: minor conscious intervention

Maximum numbers approved (for the Full Approval Duration):

Species	Strain	Age/Sex/Weight	Total	Supplier/Source
02: rat	wistar	5weeks/male/>150g	60	**ARC Perth or transferred from other approved protocols**
		TOTAL	**60**	

Location of research:

Location	*Full street address*
Central Animal House Facility	Building F9A, Research Park Drive, Macquarie University NSW 2109
ASAM	2 Technology Place, Macquarie University NSW 2109

Amendments approved by the AEC since initial approval:
1.   Administration of substances (approved June 2012)

Conditions of Approval: N/A

Being animal research carried out in accordance with the Code of Practice for a recognised research purpose and in connection with animals (other than exempt animals) that have been obtained from the holder of an animal suppliers licence.
All procedures must be performed as per the AEC-approved protocol, unless stated otherwise by the AEC and/or AWO.

This ARA remains in force until the Date of Expiry (unless suspended, cancelled or surrendered) **is contingent upon receipt of a Final Report at the end of this period (see Approval email for submission details).**

Prof Michael Gillings (Chair, Animal Ethics Committee)   **Approval Date:** 14 June 2012

D.2   SHR and WKY Ethics Approval

ANIMAL RESEARCH AUTHORITY (ARA)

MACQUARIE University

AEC Reference No.: 2012/002-9 **Date of Expiry:** 30 July 2016

Full Approval Duration: 23 February 2012 to 30 July 2016

This ARA remains in force until the Date of Expiry (unless suspended, cancelled or surrendered) **and will only be renewed upon receipt of a satisfactory Progress Report before expiry / is contingent upon receipt of a Final Report at the end of this period (see Approval email for submission details).**

Principal Investigator:
Dr Mark Butlin
Australian School of Advanced Medicine
Mark.butlin@mq.edu.au
0422 908 895

Associate Investigators:
Albert Avolio	0408 657 616
Zahra Kouchaki	0403 491 774
Mojtaba Golzan	0451 053 403
Simon McMullan	0402 073 146

Other People Participating:
Dana Georgevsky	0422 122 996

<div style="border:1px solid red">

In case of emergency, please contact:
the Principal Investigator / Associate Investigator named above
or Manager, CAF: 9850 7780 / 0428 861 163 and **Animal Welfare Officer**: 9850 7758 / 0439 497 383

</div>

The above-named are authorised by MACQUARIE UNIVERSITY ANIMAL ETHICS COMMITTEE to conduct the following research:

Title of the project: Effect of acute baroreceptor stimulation on aortic haemodynamics.
Purpose: 4 - Research: Animal or human biology
Aims: This project aims to investigate the effect of a device which stimulates the barorecptors, on the sympathetic outflow of the brain and the stiffness of the aorta in rats.
Surgical Procedures category: 2 – Animal Unconscious without Recovery

All procedures must be performed as per the AEC-approved protocol, unless stated otherwise by the AEC and/or AWO.

Maximum numbers approved (for the Full Approval Duration):

Species	Strain	Age/Sex/Weight	Total	Supplier/Source
02 - Rat	WKY	10-35 weeks/~250g-450g /male	64	ARC Perth
02 - Rat	SHR	10-35 weeks/~250g-450g /male	64	ARC Perth
		TOTAL	128	

Location of research:

Location	Full street address
Central Animal Facility	Building F9A, Research Park Drive, Macquarie University NSW 2109
ASAM	Building F10A, 2 Technology Place, Macquarie University NSW 2109

Amendments approved by the AEC since initial approval:

1. *Amendment #1 - Addition of Zahra Kouchaki as Associate Investigator (Approved February 2013).*
2. *Amendment #2 - Extend approval duration by 2 years (Approved February 2013).*
3. *Amendment #3 - Removal of Mr George Lindesay and addition of Dr Mojtaba Golzan as Associate Investigator (Exec Approved 6 February 2014, ratified by the AEC 20 February 2014).*
4. *Amendment #4 - Amendment to procedure – Imaging of vessels in the eye of the hypertensive and normotensive animals whilst they are anaethetised (Approved 20 Feb 2014).*
5. *Amendment #5 - Addition of Dana Georgevsky as Research Assistant (Exec Approved 6 May 2014, ratified by AEC 15 May 2014).*
6. *Amendment #6 - Experimental design - age at which animals are studied (Approved 19 June 2014).*
7. *Amendment #7 - Request of extension until 10 June 2015 (Approved by AEC 19 February 2015).*
8. *Amendment #8 – Extension to approval duration until 30 September 2015 (Approved by Exec, ratified by AEC 18 June 2015).*
9. *Amendment #9 – Addition of Dr Simon McMullan as Associate Investigator (Approved by Exec, ratified by AEC 18 June 2015).*
10. *Amendment #10 – Extend approval duration to 30 July 2016 and additional 32 animals (Approved by Exec. Ratified by AEC 17 September 2015).*

Conditions of Approval: N/A

Being animal research carried out in accordance with the Code of Practice for a recognised research purpose and in connection with animals (other than exempt animals) that have been obtained from the holder of an animal suppliers licence.

Professor Mark Connor (Chair, Animal Ethics Committee) **Approval Date:** 17 September 2015